

FACILITY FORM 602

N71-20630

(ACCESSION NUMBER)

(THRU)

(PAGES)

(CODE)

NASACR-111877

(NASA CR OR TMX OR AD NUMBER)

(CATEGORY)

NASA CR-111877

TECHNICAL REPORT

AN EXPERIMENTAL INVESTIGATION AND EVALUATION OF A DOPPLER RADAR TECHNIQUE FOR THE MEASUREMENT OF THE FLOW GENERATED BY WING TIP VORTICES

By: William W. Joss, Hendrik W. Prinsen, Calvin C. Easterbrook

FILE
CASE COPY

CAL No. AF-3015-C-1

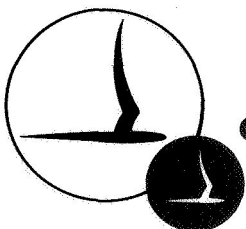
Prepared for:

National Aeronautics and Space Administration
Langley Research Center
Hampton, Virginia 23365

FINAL SUMMARY REPORT

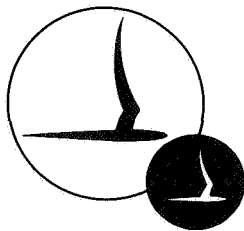
Contract No. NAS-1-10290

20 January 1971



CORNELL AERONAUTICAL LABORATORY, INC.

OF CORNELL UNIVERSITY, BUFFALO, N. Y. 14221



NASA CR-111877

CORNELL AERONAUTICAL LABORATORY, INC.
BUFFALO, NEW YORK 14221

AN EXPERIMENTAL INVESTIGATION AND EVALUTION OF A
DOPPLER RADAR TECHNIQUE FOR THE MEASUREMENT
OF THE FLOW GENERATED BY WING TIP VORTICES

By:

William W. Joss, Hendrik W. Prinsen
Calvin C. Easterbrook

CAL NO. AF-3015-C-1

FINAL SUMMARY REPORT


Prepared for:

National Aeronautics and Space Administration
Langley Research Center
Hampton, Virginia 23365


Contract No. NAS 1-10290

20 January 1971

PREPARED BY:


W.W. Joss
Project Engineer

APPROVED BY:


G.M. Cash
Dept. Head
Aerosystems Research

ABSTRACT

This report describes results of tests conducted to determine if radar reflective chaff injected at the wing tip of an aircraft would be ingested into the vortex structure and sufficiently distributed to allow velocity profiles to be measured by a Doppler radar. The results are presented in the form of flow field visualization results and an analysis of radar returns.

ACKNOWLEDGMENTS

Technical assistance and guidance was provided by G. M. Cash of the Aerosystems Research Department. B. R. Tripp and S. N. Andre of the Electronics Research Department made significant contributions in the area of radar technology and data processing. The piloting responsibilities during the flight tests were capably handled by M. L. Parrag and other members of the Flight Research Department. The efforts of G. C. Vorie in operating the radar and D. O. Bliven during the test program are sincerely appreciated.

This study was performed under the technical supervision of Mr. R. E. Dunham of the Langley Research Center, NASA.

W. W. Joss
H. W. Prinsen
C. C. Easterbrook

CONTENTS

<u>Section</u>		<u>Page</u>
	ABSTRACT	ii
	ACKNOWLEDGMENTS	iii
1	INTRODUCTION	1
2	ANALYTICAL CONSIDERATIONS	3
3	EXPERIMENTAL APPARATUS	7
	A. Short-Pulse Doppler Radar	7
	B. Chaff and Chaff Dispensing Apparatus	9
	C. Flight Test Set-Up	10
4	RESULTS AND DISCUSSION	12
	A. Preliminary Discussion	12
	B. Analysis of Radar Data	14
5	CONCLUSIONS AND RECOMMENDATIONS	18
	REFERENCES	20
	TABLES	21
	FIGURES	

1. INTRODUCTION

Predictions of the characteristics of the wing-tip vortices generated by large aircraft, especially their position, maximum azimuthal velocities and dissipation rates, have assumed increasing importance in connection with wake encounters in the terminal zones around major airports. This is particularly true when aircraft of substantially different size are required to operate in close proximity during approaches and departures. Accurate wake predictions require, however, the existence of a suitable analytical model and this, in turn, depends on the availability of accurate experimental measurements of vortices generated under variable, but closely controlled conditions. Such measurements must take into account not only the presence of the wing-tip vortices, but also those which originate, for example, at the ends of the flaps or at the wing-body juncture.

Various measurement schemes have been proposed and applied in previous programs, usually with a limited degree of success. These methods have included low-altitude tests^{1,2} in which measurements were made as the vortices drifted past highly instrumented towers, as well as high altitude tests^{3,4,5,6} involving flights directly into wakes. There are several disadvantages associated with these direct probing techniques. Tower mounted probes can generate significant disturbances in the vortices as the core passes over the tower. This leads to some uncertainty in the interpretation of detailed, localized measurements. In addition, it is difficult to repeatedly and consistently cause the vortices to drift over the towers at a given time after passage of the airplane. Finally, unless the tower were exceptionally tall, all measurements would necessarily be made while the vortices were in ground effect. This may lead to significant changes in the dissipation and break-up phenomena, especially if the tests were conducted in the presence of crosswinds or low-level turbulence.

Airborne measurements are generally made by flying one aircraft into the wake of another. Besides the obvious problem of accurately locating the center of the wake, the measurements must be corrected to account for

the motions, often large, induced on the penetrating aircraft. The extent to which the wake is disturbed by the penetrating aircraft in the process of making the measurement is unclear, and has usually not been considered.

Because of the difficulties associated with the methods discussed above, an alternative technique designed to provide an interference-free measurement at relatively long distances and high altitudes has been conceived. This technique utilizes a high resolution, coherent pulse-Doppler radar to measure the position and velocity of radar chaff injected directly into the flow near the wing tip of an aircraft in flight. If the chaff particles were to be entrained and held by the vortices, knowledge of the chaff behavior would lead directly to an understanding of the behavior of the vortices.

The success of the method depends on satisfying two basic criteria. First, the chaff which is injected into the wake must have adequate radar reflectivity to permit the radar measurements. Second, the chaff must remain in the high velocity region of the vortex long enough to allow the velocities, positions and dissipation rates of the vortices to be determined. These are somewhat conflicting requirements. The present study was undertaken in order to develop a background with regard to these criteria and establish the feasibility of the proposed measurement technique. The basic question to be answered dealt mainly with the interaction of the chaff with the vortex. Specifically, information was sought regarding the ability of a wing tip vortex to entrain and hold chaff so that radar measurements could be made on the vortex. The study was, of necessity, largely experimental. That is, since the basic mathematical model of the vortex flow is still rather in doubt, the results of a purely analytic study would be of marginal value. Therefore, a direct flight test program, utilizing an existing short pulse Doppler radar, was undertaken. This report describes the results obtained by the study.

2. ANALYTICAL CONSIDERATIONS

It is well known that a force must be continuously applied to a body in order to cause it to follow a curved (i. e. , inwardly accelerated) path. In the case of a parcel of air traveling around a nearly circular path in a vortex, this necessary inward force is supplied by the existing pressure gradient. If a test particle with a density different than air were injected into such a vortex pattern, its trajectory would not follow that of the air. That is, if the particle were heavier than air, it would tend to be thrown outward. If it were lighter than air, say, for instance, a helium-filled balloon, it would be forced inward. At first glance, then, it would seem that solid chaff particles, many times heavier than air, could never remain close to the center of a vortex. However, this conclusion is not true in general, as is demonstrated through observations of naturally occurring vortices. In particular, tornadoes, dust devils, and waterspouts can pick up and entrain large solid objects or particles for long lengths of time. These particles often appear to rotate about the axis of the vortex in a circular motion, forming a cylinder about the core. This implies that certain stable, discrete, orbits must exist for these particles. In addition to drawing these particles inward, the vortices are often seen to accelerate the objects axially. These two motions in the vortex, i. e. , the radial inflow associated with the initial inward motion of the particles and motion along the axis, are intimately connected. Unfortunately, they are often ignored in simplified models of the flow. However, this should not be taken to imply that their existence is unimportant when considering the detailed behavior of the vortices. In studying the interaction of chaff particles with the flow in a wing-tip vortex, the radial inflow becomes a crucial factor. It is this inflow and the associated drag it produces on the chaff particles which allows the particles to be entrained by the wing-tip vortex. This phenomenon is well illustrated, for instance, by the behavior of dense smoke particles near a vortex. Recent NASA films¹ strikingly demonstrate the strength and persistence of the axial and radial motions as smoke is drawn into the regions near the core.

The centrifugal force acting on such particles can be related to the observed motion of the particle as follows:

$$\frac{F}{W} = \frac{V_\theta^2}{r g} \quad (1)$$

Here, F is the centrifugal force, W , the weight of the particle, V_θ , the instantaneous tangential velocity, r , the instantaneous radius of curvature, and g , the acceleration of gravity.

If the particles are moving around the vortex in a steady circular path, the centrifugal force must just be balanced by the drag force produced by the relative motion of the inwardly spiraling air, i. e. ,

$$F = D = \frac{1}{2} \rho V_R^2 C_D A \quad (2)$$

Here, D is the drag, ρ , the air density, V_R , the inward radial component of the relative velocity, C_D , a drag coefficient, and A , an appropriate area. This expression can be simplified by relating the relative velocity to the terminal velocity of the particle. That is, when a particle is falling at its terminal velocity, its drag just equals its weight. Ignoring changes in the drag coefficient as a function of velocity, the drag must vary as the square of the velocity. Therefore, the drag can be given by

$$D = W \left(\frac{V_R}{V_t} \right)^2 \quad (3)$$

where V_t is the terminal velocity.

Using equation (3), the balance of forces can be written

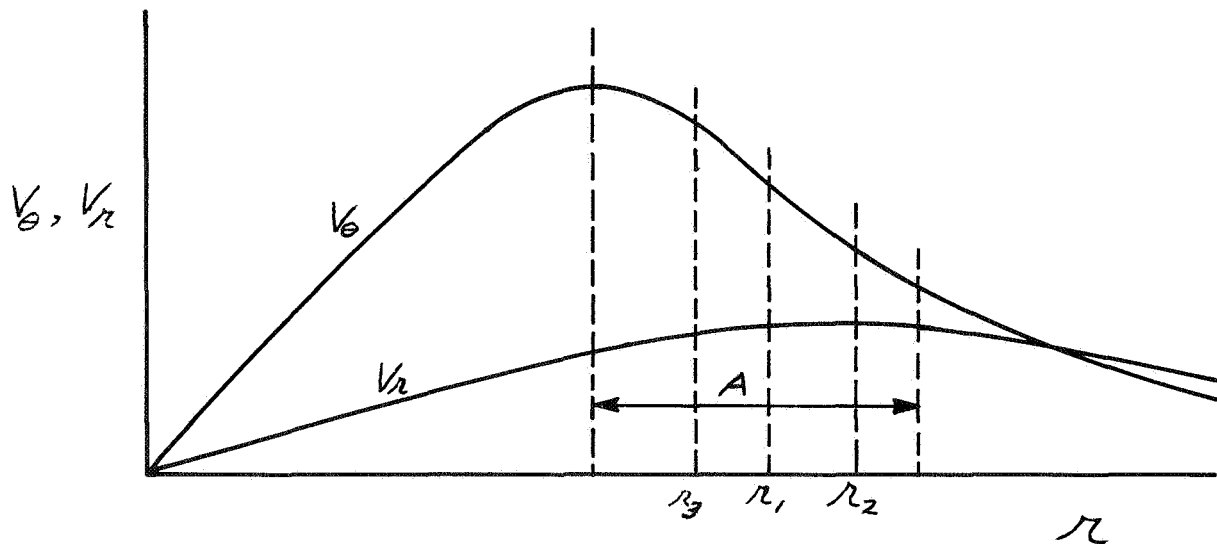
$$F = D = W \left(\frac{V_R}{V_t} \right)^2 \quad (4)$$

Combining equations (4) and (1)

$$\frac{F}{W} = \frac{V_\theta^2}{r g} = \left(\frac{V_R}{V_t} \right)^2 \quad (5)$$

This expression relates the required particle terminal velocity for a circular motion to the tangential and inward radial velocity components. However, this criterion must be supplemented by a further criterion dealing with the stability of such a balance of forces. That is, unless the particle is in stable equilibrium, a uniform circular motion will never result.

The existence of a mechanism to provide the required stable orbits observed in practice is suggested by the experimental work of Ying and Chang.⁷ They show that in a laboratory-generated vortex, the maximum radial inflow velocity occurs at a larger radius than the maximum tangential velocity. This situation is illustrated in the following sketch:



TANGENTIAL AND RADIAL VELOCITIES IN A VORTEX AS A FUNCTION OF RADIUS (YING AND CHANG)

Consider the behavior of a particle placed in region A. If at r_1 , the terminal velocity is such that Equation (5) is satisfied, the forces on the particle will be instantaneously balanced. Now, suppose the particle moves to a larger radius, r_2 . We see that the tangential velocity decreases, hence, the centrifugal force decreases. (This decrease is further enhanced by the increase in radius.) At the same time, the radial inflow velocity and the drag on the particle increase. Therefore, as the centrifugal force decreases and the (inwardly directed) drag increases, the particle experiences a net inward, or restoring, force. The converse is true if the particle had moved to a smaller radius, say r_3 . Region A may not necessarily be the only region where such a stable orbit is possible. In fact, using the analytical expressions given by Ying and Chang for the velocity components, one finds stable orbits at any radius where the particle's terminal velocity is such that Equation (5) is satisfied. Although the expressions of Ying and Chang may be slightly idealized, they lend support to the idea that stable orbits may be found over large regions in the vortex. Additional evidence includes yet unpublished results recently obtained at the Cornell Aeronautical Laboratory which have shown that very thin filaments are entrained by a vortex generated in a 4 foot diameter chamber.

In summary, chaff particles with a terminal velocity which is low enough to satisfy Equation (5) could be held in the vortex by the inwardly directed radial velocity component. As long as the velocity profiles are such that, with an increase in radius, the centrifugal force decreases more rapidly than the drag due to the inward velocity, the balance of forces is stable and the chaff particles should rotate steadily about the vortex.

3. EXPERIMENTAL APPARATUS

The experiments to be discussed in the following sections made use of a short pulse, coherent Doppler radar developed by Cornell Aeronautical Laboratory under Laboratory support.⁸ For these tests, the radar was located at the Cornell radar facility in Newstead, New York. During the tests, chaff was dispensed from the wing tips of an Aztec aircraft owned and operated by CAL. The aircraft flew through the vertically directed radar beam at low altitude in such a way that the chaff-vortex system would drift back over the radar. The behavior of the chaff was then studied in detail as it moved through the beam. A more extensive discussion of each of the experimental factors is given in the following sections.

A. Short-Pulse Doppler Radar

The important characteristics of the short pulse Doppler radar used in this investigation are summarized in Table 1. A more detailed description of the radar system can be found in the above reference. A block diagram is shown in Figure 1. For the tests described here, the radar was used to measure the backscatter from chaff particles occupying three independent range cells, as illustrated in Figure 2. The short pulse (≈ 1 nanosecond) transmitter and receiver range gating provided a range resolution of approximately six inches. The volume of each resolution cell is determined by the beamwidth of the radar antennas (10°), the depth of the radar resolution cell (1/2 ft), and its range. The range gate separation used was 50 feet. For these tests, the antennas were pointed vertically upward and each range gate swept a distance of 50 feet during a one-second time period. Thus, during one sweep the three range gates covered adjoining altitude intervals extending from 75 to 125 feet, 125 to 175 feet, and 175 to 225 feet respectively. The output signal from each range gate is centered at a frequency of 50 kHz. The amplitude of the signal is proportional to the amplitude of the received, Doppler-shifted, microwave signal. Doppler

shift is reflected as a frequency shift of the output signal from a stable 50 kHz reference frequency. The latter is generated in the radar using frequency stable crystal controlled sources. The outputs of the three range gates during the tests were recorded on magnetic tape together with a range sweep timing signal and the 50 kHz reference signal. Upon playback, the range sweep timing signal (1 Hz sweep rate) provides the necessary information for correlating the recorded radar range gate outputs with the range gate positions. The 50 kHz signal provides the reference for determining the Doppler shifts of the received signal.

As indicated earlier, the radar targets in these tests consist of individual scatterers (chaff) located within the three radar range cells. If the scatterers were stationary in space and if the range cells were not being swept, the received signal would be constant in amplitude. With a sweeping range gate, the signal varies in amplitude according to the varying numbers of scatterers distributed within the radar range cell at any particular time. The maximum frequency of these amplitude or envelope variations will, with a sweep rate of 50 ft/sec and a range cell width of 0.5 feet, be limited to approximately 100 Hz.

If, in addition, the scatterers in the radar range cell are in motion relative to one another, then the rate at which the relative phases of the scatterers change will produce additional fluctuations in the intensity, or the envelope, of the received signal. The rate at which the envelope of the radar signal crosses its average value gives an indication of the width of the velocity spectrum of the scatterers. This width can be approximated⁹ as:

$$\sigma_u = \frac{\overline{\pi_o} \lambda}{5.22} \quad (6)$$

Here σ_u is the standard deviation of the velocity spectrum, $\overline{\pi_o}$ is the mean rate at which the signal envelope crosses its average value, and λ is the radar wavelength. When the scatterers in the range cell also have a "mean" velocity with respect to the radar, the received signal will of course exhibit a Doppler shift corresponding to the mean velocity.

B. Chaff and Chaff Dispensing Apparatus

The chaff used for these tests consisted of cylindrical filaments, or dipoles, of four different diameters. All of the dipoles were cut approximately one-half wavelength long, at X-band, in order to maximize their radar reflectivity. The four different sizes of chaff are shown in Figure 3. The chaff on the far left had a diameter of 3.5 mils and consisted of nylon filaments coated with a thin layer of silver. As seen, the bundles, which contained approximately 45,000 individual filaments, were loosely held by a paper band. The three chaff bundles on the right contain aluminum coated fiberglass filaments. Each bundle contains 115,000 filaments with diameters of 1.5, 1.0 and 0.7 mils respectively. These bundles were rather tightly packed, as illustrated by the partially expanded bundle of 1.5 mil chaff shown at the bottom of the figure.

The chaff filaments had measured terminal velocities which varied as follows:

<u>Diameter (mils)</u>	<u>Terminal Velocity (fps)</u>
3.5	2.0
1.5	1.0
1.0	0.7
0.7	0.5

The nearly linear dependence of the terminal velocity on chaff diameter is due to the decrease of the drag coefficient as the Reynolds number increases in this range.

Initially, the chaff was ejected by three identical dispensers, one of which is shown in Figure 4. In this device, a piston, driven by an electric motor through a rack-pinion gear assembly, forced the chaff from barrels which were screwed into place at the end of the channel. The three different inside-diameter liners were preloaded with the appropriate size chaff bundles and then held in place inside the large barrels by set-screws. The chaff was loaded by dropping the wrapped bundles into the slightly oversized liners and then unwinding the binding string by pulling on one end. The major portion of the apparatus was mounted inside the wing tip of the Aztec. The barrels

were then screwed into place during the tests by inserting them through the dispensing ports in the upper surface of the wing. The arrangement of the three dispensing ports is shown in Figure 5. The ports were located approximately two-thirds of a chord length from the leading edge with the outermost port 15 1/2" in from the wing tip. This location was selected on the basis of flight tests utilizing tufts on the upper surface of the wing and streamers attached to the trailing edge. These tests clearly revealed the location of the vortex as it left the wing.

Also visible in Figure 5 is an explosive dispenser protruding from the inboard port. This dispenser was used to minimize the problem of chaff clumping, to be discussed later. The dispenser was essentially a hollow tube which fit into the regular chaff barrel. The chaff was expelled by a 1/2 gram charge of black powder ignited by an electrically activated squib.

In addition, a wing-mounted flare rack, extending behind the trailing edge, was also used to dispense the chaff. This rack, shown in Figure 6, was first used during some earlier preliminary tests. An electrically activated charge expels the chaff from the barrels. The rack was used during the present series of tests to further study the effect of the dispensing techniques on the problem of chaff clumping.

C. Flight Test Set-Up

As indicated earlier, the flight tests were conducted at low level, approximately 200 feet, over CAL's Newstead, N.Y., radar site. An FAA waiver was obtained for the operation. During the runs, the aircraft was flown at 90 mph with the flaps up, in order to produce as strong a vortex as possible. The runs began at a preselected initial point, which was approximately two miles downwind from the radar. A portable VHF transceiver was used to communicate with the aircraft during the tests in order to simplify alignment of the flight path and the timing of the chaff release.

Two other receivers were used to coordinate with the radar operator and camera personnel. Numerous photographs were taken during the runs, primarily to record the aircraft altitude, measured with a vertical marker as shown in Figure 7, and to record the behavior of the vortex. A

visual tracer technique was devised using red Day-glo paint pigment. The pigment was mixed with talcum powder and ejected from one of the chaff dispensers as chaff was simultaneously being ejected from another dispenser. In spite of the fact that the phosphorescent pigment was quite easy to see, it was very hard to photograph. After trying Polaroid film and 35 mm color and high contrast black and white film, it was found that a 70 mm Hasselblad camera using a red filter and Kodak Aerocon film gave a reasonable image of the pigment. Figure 8 was obtained during an especially low pass made in order to illustrate the technique. The typical cylindrical laminar structure of the vortex can be seen forming at the downstream end of the trace. Generally, the visual tracer could be seen up until the point of vortex breakdown. Occasionally, this took as long as 35-40 seconds.

An instrumented tower was used to measure temperature and wind speed and direction during the runs, up to 50 feet over the surface. This was done primarily to assure that strong windshear or instabilities were not present at the lower altitudes. Most runs were made with winds of 5 mph or less, a necessity since the radar beam was only approximately 40 feet wide at the nominal test altitude. A 10 mph wind, for instance, would cause a given particle to drift completely through the fixed beam in approximately 3 seconds.

This problem could have been alleviated if the existing radar were to have been modified to provide a tracking capability. This was, however, beyond the scope of the present study.

A helium filled weather balloon with streamers attached was tethered at approximately a 200 foot altitude alongside the flight path, to check for crosswinds aloft. This was very important since the technique required flying directly into the wind over the radar and releasing the chaff on the upwind side of the beam. Any unknown cross wind could, therefore, cause the chaff to miss the beam. This was especially important when the chaff release was delayed in an attempt to let the vortex "age" before it passed through the beam. Figure 9 shows the Aztec on a typical run, passing over the trailer housing the radar just prior to a chaff release.

4. RESULTS AND DISCUSSION

A. Preliminary Discussion

Flight tests were conducted on 10 separate days, during which some 67 passes were made over the radar. Chaff was released during 48 of these trials and radar data were obtained on 38 runs. It became very evident from the radar returns obtained during the early runs that the chaff was not being drawn into a purely cylindrical pattern, as was the visual tracer, for example. In fact, the radar return appeared to be spread out vertically over a distance of about 50 feet. A careful search of the ground beneath the flight path revealed that a substantial amount of the chaff was reaching the ground in clumps similar to that shown on the left in Figure 10. The most reasonable explanation of the vertically distributed radar return was that the falling chaff bundles were trailing off individual groups of filaments which fell at a much lower speed and, thereby, became distributed over a large distance.

It was found that in several cases, the thin paper separators placed between the chaff bundles during loading were remaining with the bundles right down to the ground. They were apparently acting as windshields during the ejection process and were preventing the chaff packages from being broken up by the flow over the wing. Removal of these separators led to some apparent improvement in the dispersal, as judged from the aircraft, but it was obvious that clumping was still occurring. The next step involved beveling the ends of the barrel liners shown in Figure 4, i. e., cutting off the ends of the liners at an angle. The liners were also allowed to protrude very slightly above the wing surface. This change meant that as the chaff packages reached the end of the tube, the filaments would be released over a longer distributed time period. Thus, those filaments on the shorter, upwind side of the tube would be released before those on the opposite side. A series of flights were then made during which chaff was released by both types of dispensers. A Fastax movie camera was mounted in the aircraft cabin and films of the dispensing process were taken at approximately 1000 frames per second.

These films showed that the original scheme allowed the bundles to emerge to a large extent still intact. The bundles then tumbled back along the wing surface under the action of the shear flow in the boundary layer, with some filaments streaming off in the process. The tumbling seemed to lead to the matting and clumping which had been observed. The beveled dispensers seemed to correct this problem to a large extent although dense groups could still be seen leaving the tube at intervals. The diameter of the chaff filaments seemed to have some effect on the clumping, with the small diameters tending to be worse than the large diameters.

The explosive dispenser, described earlier, was also tested. The chaff bundles left the end of the tube at an apparent speed exceeding 500 feet per second and the details of the breakup process could not be observed. From the ground, however, it was possible to see that the clumps which were formed were moving around the vortex instead of falling out as was observed when the chaff was dispensed by the piston-cylinder arrangement. It, therefore, seemed reasonable to expect that smaller, invisible clumps and any single filaments were in fact being entrained by the vortex. The same type of phenomenon was observed when the chaff was dispensed from the wing-mounted flare rack.

There was some concern that the flare rack might substantially alter or destroy the uniform vortex flow behind the wing. However, observation of the visual tracer seemed to indicate that there were no apparent differences between the vortices from either tip. Figure 11 shows the pattern formed by the pigment behind the wing rack. The photo was taken very shortly after the passage of the aircraft. The aircraft flew through from right to left and two tubes of pigment were dispensed sequentially. The tracer on the right appears to be growing to the left, or upstream, while that on the left is still in the process of formation.

Since the chaff was still not being entirely drawn into a thin cylinder around the vortex, it became apparent that studying only the spatial distribution of the radar return would not, as had originally been thought, indicate

whether or not a large amount of chaff was being entrained by the vortex. The ideal situation would, of course, have been the appearance of a radar return from the chaff corresponding to the visual observations of the pigment. The radar return, when combined with the visual observations of the pigment entrained by the vortex, did, however, show that there definitely was chaff at the same altitude as the vortex. Therefore, a more detailed analysis of the data was called for. That is, although the chaff entrained by the vortex was surrounded by other chaff falling freely, it was felt that an analysis of the Doppler return within the overall chaff cloud should provide a means of distinguishing the return generated by the vortex. This analysis was performed and is described in the next section.

B. Analysis of Radar Data

The tape recorded Doppler signal time histories were played back through an oscilloscope and photographed. Figures 12 to 15 show representative samples of such signals as a function of range for typical runs. In these figures, each of the two horizontal traces represents a fifty-foot altitude interval, which is swept once per second. The vertical extent of the chaff return is clearly evident in these photographs.

In order to obtain more information on the detailed structure of the radar return, expanded recordings of the signal time histories were obtained by mixing the received signal, which is centered at 50 kHz, with a 49 kHz signal. The resultant product, a signal centered around 1 kHz, was recorded directly on a fast oscilloscope chart recorder. The radar reference frequency of 50 kHz was translated in the same way and simultaneously recorded. A block diagram of this processing technique is shown in Figure 16. A chart speed of 60 inches per second was used so that the time history obtained during each one-second sweep of the range gate was expanded over a chart length of 60 inches. The expanded scale thus allows observation of the signal over small range increments (6 chart inches \approx 5 foot radar range). The Doppler shift information can be extracted by a direct comparison of the frequency of the received signal with the recorded reference signal.

Inspection of these expanded records immediately revealed an important distinction between different runs. For several runs, many consecutive sweeps exhibited certain clearly defined range intervals extending over 8 to 10 feet within which the return was distorted and the amplitude varied much more rapidly than at all other ranges on the same trace. These extremely rapid variations in signal amplitude, which result from a large spread in the frequency of the returned signal, indicate that, as explained in Section III-A, the scatterers have a large relative motion with respect to each other. This is a clear indication of the presence of the vortex. Where there is no such strong relative motion, the envelope of the returned signal is smooth and well defined. The smoothly varying signal amplitudes for these sweeps are attributed solely to the spatial variations of the radar cross section of the chaff.

Figures 17 to 20 illustrate the two basically different types of returns which were observed. Figures 17 and 18 represent portions of the traces obtained from runs 19a and 54 where there were no strong indications of the presence of the vortex. In these traces, the envelope of the signal is smooth and well defined. In contrast, Figures 19 and 20, obtained from runs 47 and 56a, show the distinct distortions in the signal which can be associated with the large Doppler spreads generated by the vortex. In particular, attention is drawn to Figures 20a and 20c where the abrupt change in the character of the signal is clearly evident mid-way through the traces.

A brief analysis was made of the velocity spread associated with the disturbed regions of runs 47 and 56a, as well as for several regions from runs 19a and 54. Over a small range section, representing approximately 1 foot, the number of zero crossing of the signal envelope around its average value were estimated and, using Equation (6), the corresponding spread calculated. Also, for all four runs the mean velocity of the composite target along the direction of the radar beam was estimated from the mean Doppler shift. The results are shown in Table II. The significant difference in the velocity spread between the two pairs of runs is noted. This can only be ascribed to chaff being retained in the vortex after the aircraft had passed overhead, in the one case, and the absence of significant

amounts of chaff in the vortex in the other case. The much smaller spreads associated with the smoothly varying signal time histories of runs 19a and 54 can be wholly attributed to spatial variations in the chaff density. It should be pointed out that the 8-10 range interval corresponding to the observed signal distortions cannot be directly interpreted as the diameter of the vortex. This is because of the spherical nature of the wavefront in conjunction with the horizontal spread of the targets within the 10° beam. In addition, the vortices were often observed to be sinuous or vertically distorted.

By increasing the sweep speed of the oscilloscope, direct expanded photographs of the signal time histories were obtained. These traces, obtained for the four runs discussed above, are shown in Figures 21 to 24. The traces differ from the strip chart recordings (i.e., Figures 17-20) in that the 50 kHz center frequency has been retained in these figures. The amplitude envelopes are thus smoothly defined in these photographs except in those regions where the large Doppler spreads distort the signal. This "hash" seems characteristic of the presence of the vortex. Through careful examination of the individual pulse shapes, it is possible to correlate the traces shown in Figures 17 to 20 with the photographs in Figures 21 to 24. This has been done and the regions on the photographs corresponding to the data displayed on the strip charts have been indicated by horizontal bars. In all, 10 runs have definitely been identified in which the large shifts associated with the vortex occur to some degree. This has been done on the basis of the strip chart recordings discussed above. In addition, several other runs show indications of "hash" on the direct oscilloscope photographs, but have not been analyzed in detail. In these runs, apparently a relatively small amount of chaff was entrained in the vortex.

After performing the direct analysis discussed above, the approximate power spectra of the signals was obtained by processing the magnetic tapes in an available spectrum analyzer. The analyzer consists of a bank of 250 filters, each having a bandwidth of 4 Hz, covering a 1000 Hz frequency band centered at 40 kHz. The outputs of the bank of filters are

integrated and then sampled 6 times per second by a rotating drum assembly. A time constant of 1/3 second (minimum for the equipment) was set in each filter channel. Each filter is sampled in sequence beginning with the low frequency end of the band. A linear sweep voltage, synchronized to the rotating drum, is generated within the equipment and serves to drive the x-axis of an oscilloscope. The output of the analyzer is connected to the y-axis of the scope.

In order to analyze the recorded radar data, it was necessary to heterodyne the 50 kHz signal down to 40 kHz to match the center frequency of the spectrum analyzer. This was accomplished by mixing the radar signal with 90 kHz and selecting the lower sideband. Selecting this difference frequency leads to a reversal in the Doppler spectrum with approaching velocities now being associated with lower frequencies rather than the reverse.

Sample spectra taken from two chaff-drop experiments are shown in Figure 25. Figure 25 a is a calibration photograph showing the noise level, a sample of the transmitted radar signal (center of sweep) and 3 frequency markers at 39.60, 40.0 and 40.20 kHz (the three large negative going signals). The Doppler transformation of the specific radar being utilized gives a 60 Hz frequency shift for a velocity of 1 meter per second. Therefore, the total sweep in each of the photographs represents 16.6 meters per second or 0 ± 8.3 meters per second with zero velocity at the central position. The amplitude as a function of frequency is displayed vertically, using a linear scale. Taking into consideration the spectrum reversal as explained above, downward velocities are to the left of center and upward velocities to the right. Figures 25 b and c represent motion in the chaff during run number 47, approximately 3 and 4 seconds after release. Note that there is a total velocity spread in excess of 11 meters per second or 35 ft per second at that time. Figures 25 d, e, and f show spectra generated from run 56a at approximately 4, 5, and 6 seconds after chaff release. Again, there is a large velocity spread of the order of 10 to 12 meters per second. The spectra shown are typical of many obtained during the chaff experiments and lend a great deal of support to the results given previously.

5. CONCLUSIONS AND RECOMMENDATIONS

The present study was undertaken in order to evaluate the use of the chaff Doppler radar technique in making measurements in wing tip vortices. Two basic criteria must be met in making such measurements. First, the chaff which is released at the wing tip must be entrained by the vortex and must follow the tangential motions of the air in the vortex. Secondly, the Doppler radar must be capable of measuring the velocity and location of the chaff within the vortex. If the chaff behaved ideally, the filaments would move around the vortex in stable, discrete orbits. The radius of the orbit would depend on the terminal velocity of the particular type or size of the chaff chosen. This radius could then be measured by the radar and the velocity at a particular radius determined. At the same time, the motion of the vortex could be measured and the dissipation, or decay period, determined. Both of these points are important in terms of metering aircraft in the ATC environment.

The experimental results obtained in the present program, using a short pulse Doppler radar, have clearly shown that individual chaff filaments dispensed at the wing tips of an Aztec aircraft are, in fact, entrained by the wing tip vortices. An examination of the radar returns from the chaff has revealed the presence of large Doppler spreads in relatively small regions of the return. These large spreads are associated with the high velocities within the wing tip vortices. However, it was also found that a substantial percentage of the chaff which was released from the wing tip dispensers had a tendency to form clumps which hampered the determination of the detailed velocity profiles. That is, instead of a large number of individual chaff filaments, all with a fixed terminal velocity, orbiting the vortex in a particular cylindrical shell, essentially a cloud of chaff was observed extending over a fairly broad range interval. The larger clumps fell downward, trailing off smaller clumps and individual filaments, and generally obscured the details of the behavior of the filaments actually entrained in the vortices. Primarily for this reason detailed velocity profiles could not be obtained. However, it was possible to

determine the magnitude of the velocities in the vortex and, using a delayed release technique, the change with age. This would provide valuable information in terms of applications to aircraft spacing.

The scope of the present study did not allow a full investigation of the ultimate possibility of obtaining velocity profiles by use of the chaff Doppler radar technique. However, a number of points became clear. First, the clumping problem was alleviated somewhat by changes in the dispensing procedure. Further improvements seem likely with a more extensive investigation. Secondly, the problem would be further alleviated when making measurements behind a heavier aircraft than the Aztec used in the present study. The associated stronger vortices should tend to more completely entrain the chaff clumps. Thus, further tests using a heavier aircraft and an improved dispensing system are indicated. It should be pointed out that the simple optical tracer used in the present tests proved very useful in determining the position and point of decay of the trailing vortex. It is recommended that future vortex investigations incorporate both optical and radar tracers because of the complementary nature of the two systems.

The present study also identified several desirable modifications to the Doppler radar system. For future tests, it is recommended that the Doppler radar incorporate range gate and angle tracking capability. This will facilitate measurements of the dissipation and breakup of the vortices over long time intervals. In addition, better range definition within the vortex would be obtained if the antennas were modified to produce a beam with an elliptical or fan shaped cross section. This would reduce the slant range interval over which the vortex is viewed by the radar and would assist in obtaining spatially resolved velocity measurements. Also, the number of range gates could be increased and they could be swept more slowly and over a smaller interval. This would result in longer sampling times over the vortex and would, thus, allow better definition of the vortex characteristics.

REFERENCES

1. Dunham, R.E.Jr., "Photographs of Vortex Motion," Presented at the Symposium on Wake Turbulence, Seattle, Washington, Sept. 1970
2. Garodz, L., "Measurements of the Boeing 747, Lockheed C5A and other Aircraft Vortex Wake Characteristics by Tower Fly-By Technique;" Presented at the Symposium on Wake Turbulence, Seattle, Washington, Sept. 1970
3. Caiger, B. and Gould, D.G., "An Analysis of Flight Measurements in the Wake of a Jet Transport Aircraft," Presented at the Symposium on Wake Turbulence, Seattle, Washington, Sept. 1970
4. Bisgood, P.L., Maltby, R.L. and Dee, F.W., "Some Work on the Behavior of Vortex Wakes at the Royal Aircraft Establishment," Presented at the Symposium on Wake Turbulence, Seattle, Washington, Sept. 1970
5. Condit, P.M. and Tracy, P.W., "Results of the Boeing Company Wake Turbulence Test Program," Presented at the Symposium on Wake Turbulence, Seattle, Washington, Sept. 1970
6. Andrews, W.H., "Flight Evaluation of the Wing Vortex Wake Generated by Large Jet Transports," Presented at the Symposium on Wake Turbulence, Seattle, Washington, Sept. 1970
7. Ying, S.J. and Chang, C.C., "Exploratory Model Study of Tornado-Like Vortex Dynamics," Journal of the Atmospheric Sciences, Vol. 27, No. 1, Jan. 1970
8. Young, M.C. and Tripp, B.R., "Nanosecond Pulse Doppler Radar for the Investigation of Turbulent Wakes in Shock Tunnels and Ballistic Ranges," IEEE (3rd) International Congress on Instrumentation on Aerospace Facilities, May 1969
9. Rogers, R.R., "Meteorological Applications of Doppler Radar," CAL Report, p.25, March 1964

Table 1
RADAR CHARACTERISTICS

FREQUENCY	9.2 GHz
PEAK POWER	1 W
PULSE LENGTH	1 ns (-3 dB)
PULSE REPETITION FREQUENCY	2 MHz
ANTENNA BEAMWIDTH	10° (TWO-WAY)
RECEIVER RANGE GATE DURATION POSITION	1 ns (-3 dB) VARIABLE FROM 0 TO 50 FT
RANGE RESOLUTION CELL	0.5 FT (-3 dB)
NUMBER OF RANGE GATES	3
RECEIVER NOISE FIGURE	9 dB
DOPPLER RECEIVER SENSITIVITY*	-92 dBm (S/N = 1)
RECEIVER DYNAMIC RANGE	40 dB
MINIMUM DETECTABLE DOPPLER RCS	$\sigma/\lambda^2 \approx -60$ dB

*DOPPLER SENSITIVITY FOR EQUIVALENT NOISE
BANDWIDTH : 20 kHz

Table II
DOPPLER VELOCITIES AND VELOCITY SPREADS

RUN NO.	TIME AFTER AIRCRAFT, secs	DATA POINT ALTITUDE ft	VELOCITY* ft/s	VELOCITY SPREAD ft/s
47	2	187	+17.5	15
	3	179	+ 6.5	16
	4	178	+13	15
56A	4	185	+ 3	12
	5	185	+12	13.5
	6	187	- 5	12
19A	9	157	0	2.5
	10	155	0	2.5
	11	157	0	3.5
54	4	200	0	5
	5	204	- 3	2.5
	6	204	- 5	3

*POSITIVE DOWNWARD

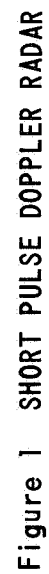


Figure 1 SHORT PULSE DOPPLER RADAR

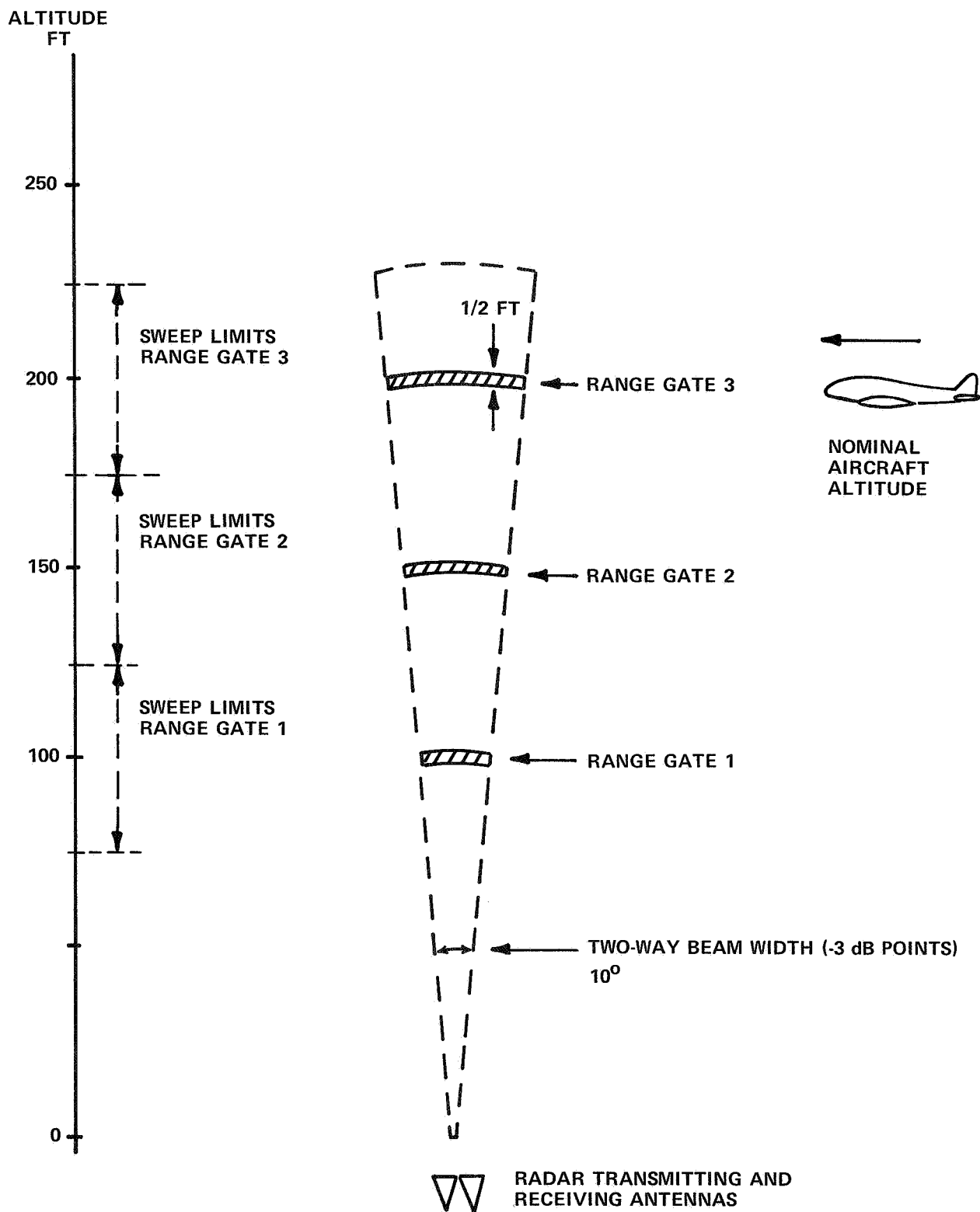


Figure 2 REGIONS SWEEPED BY RADAR

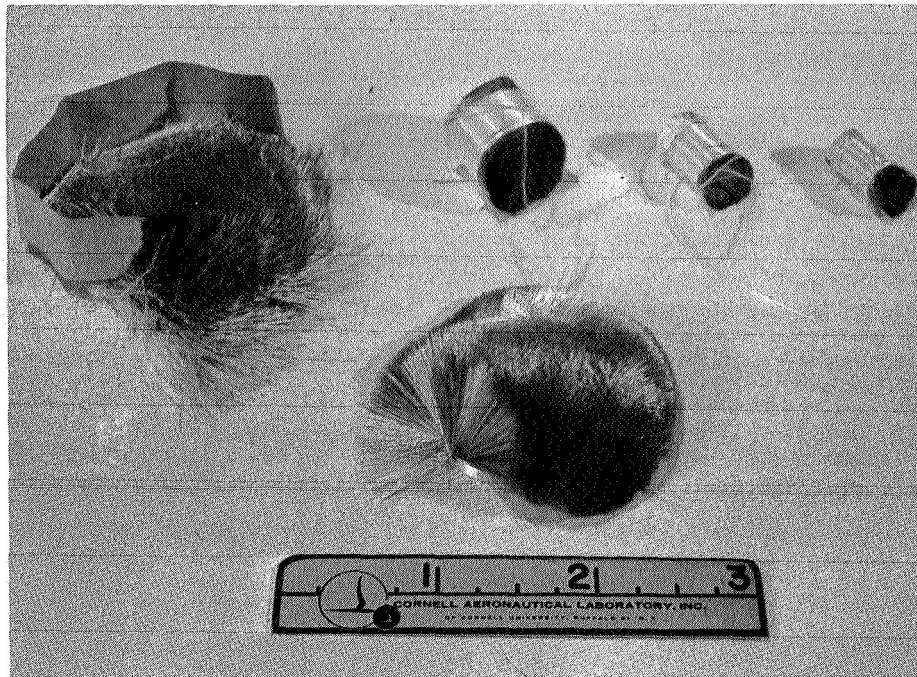


Figure 3 CHAFF TYPES USED IN TESTS

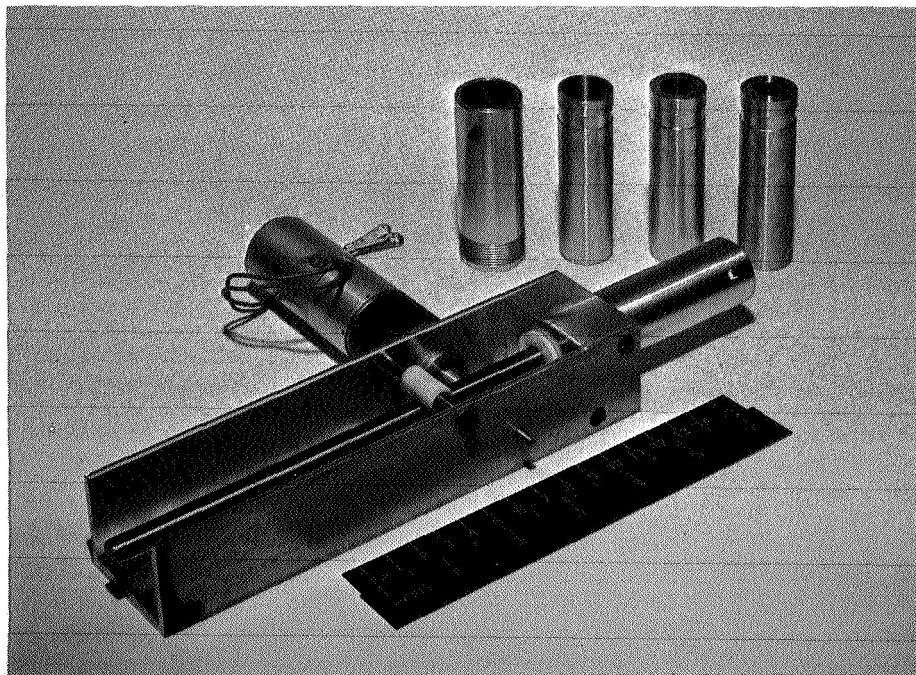


Figure 4 CHAFF DISPENSING UNIT

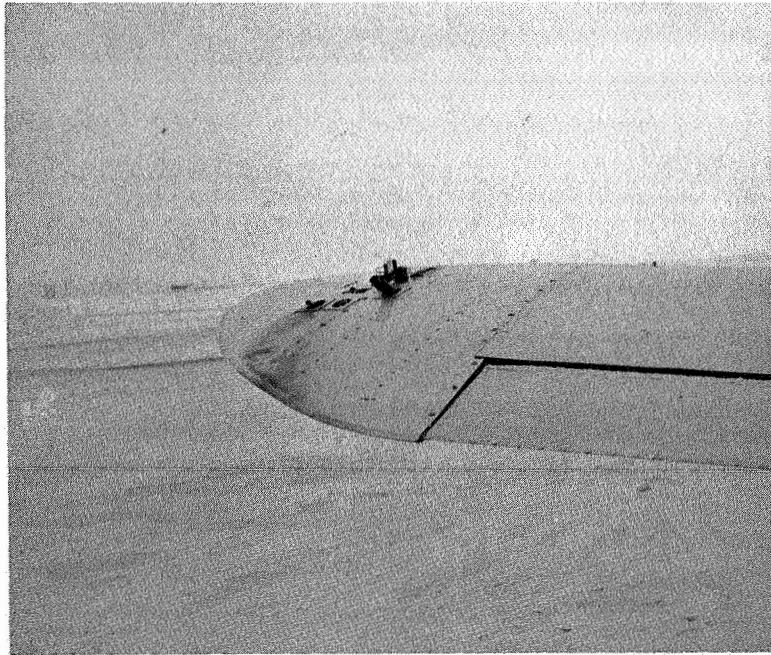


Figure 5 DISPENSING PORTS ON WING TIP

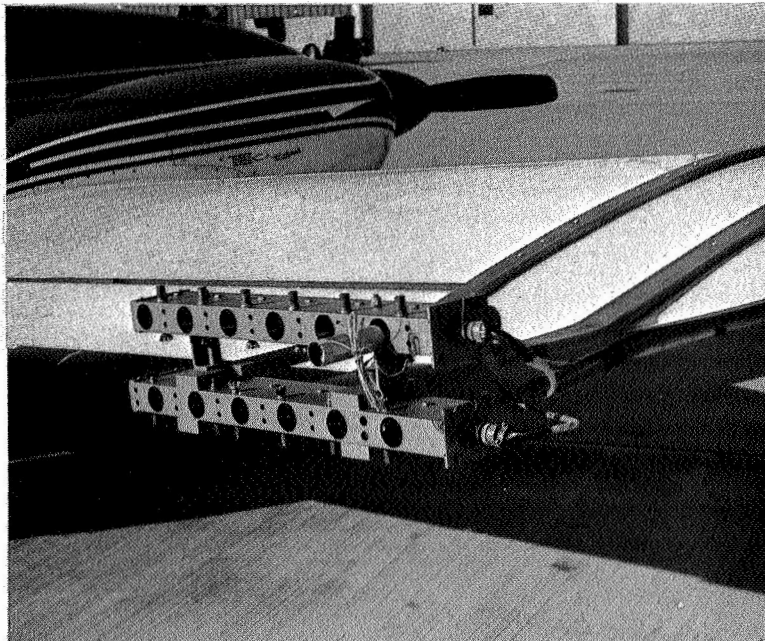


Figure 6 WING MOUNTED FLARE RACK



Figure 7 AIRCRAFT PASSING VISUAL ALTITUDE INDICATOR



Figure 8 AIRCRAFT DISPENSING VISUAL TRACER



Figure 9 AIRCRAFT APPROACHING RADAR TRAILER

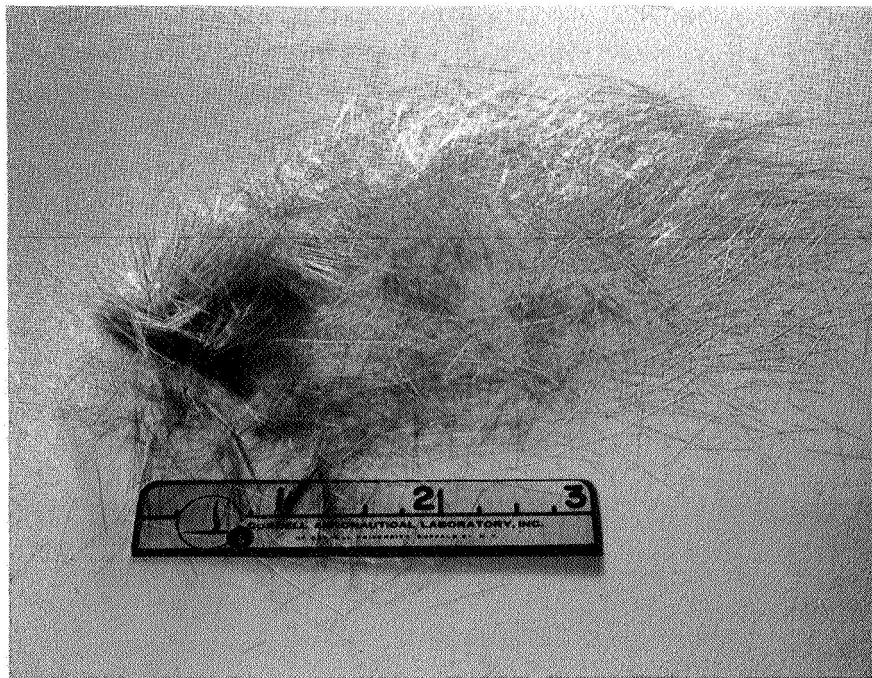
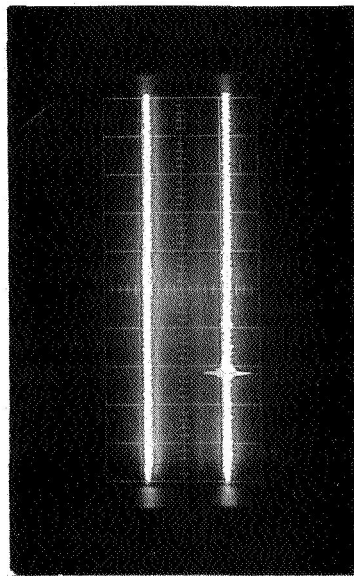


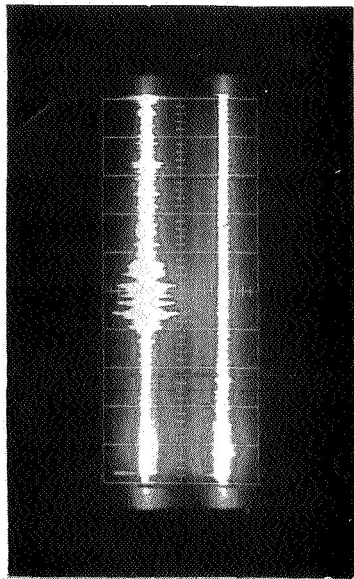
Figure 10 REPRESENTATIVE CHAFF CLUMP



Figure 11 VORTEX PATTERN BEHIND FLARE RACK

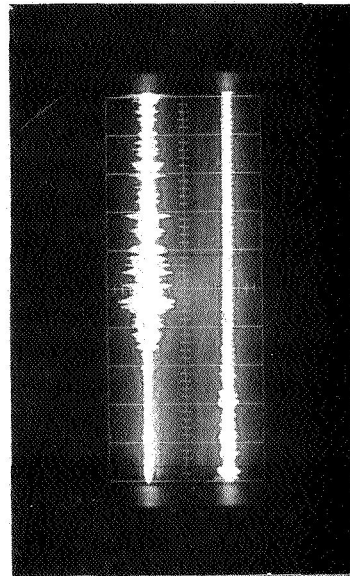


a) AIRCRAFT PASSAGE

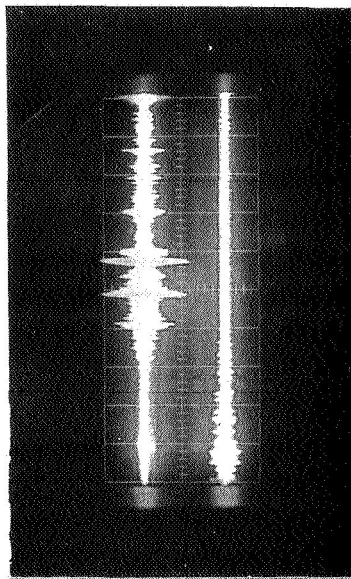


b) 9 SEC AFTER AIRCRAFT

UPPER TRACE 125 FT-175 FT
LOWER TRACE 175 FT-225 FT

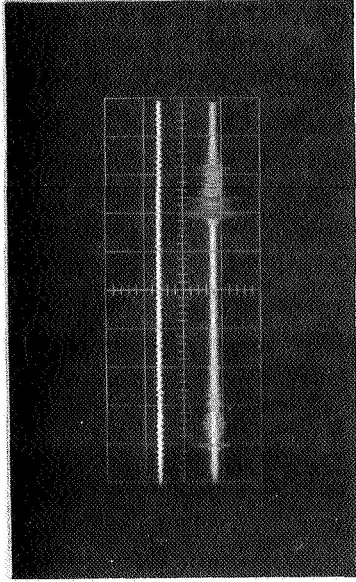


c) 10 SEC AFTER AIRCRAFT

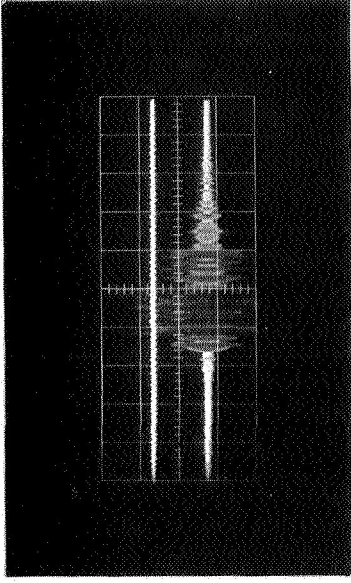


d) 11 SEC AFTER AIRCRAFT

Figure 12 RADAR RETURNS FROM RUN 19a

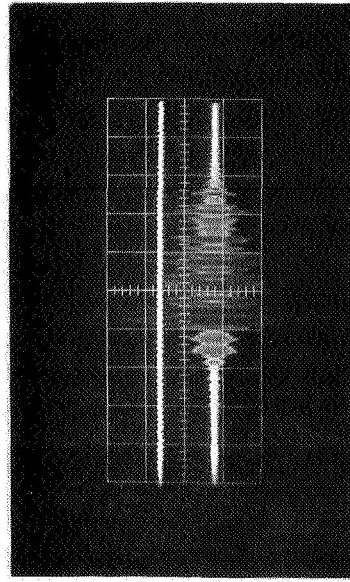


a) AIRCRAFT RETURN

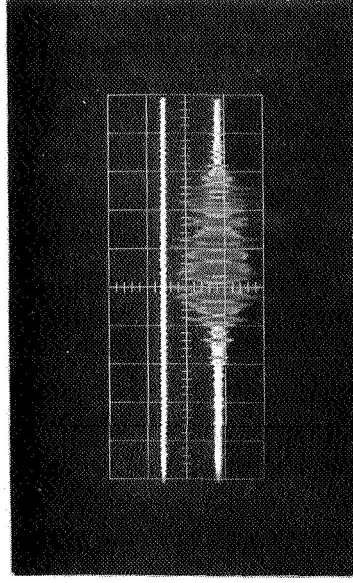


b) 4 SEC AFTER AIRCRAFT

UPPER TRACE 125 FT-175 FT
LOWER TRACE 175 FT-225 FT

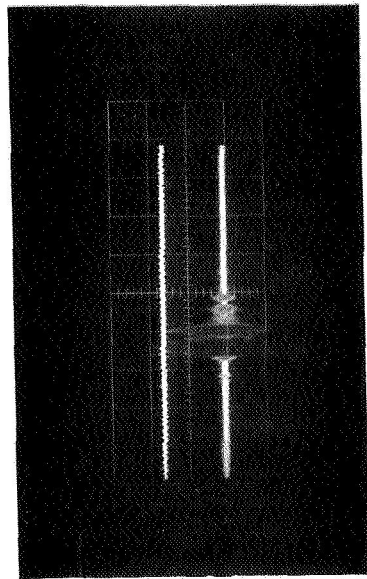


c) 5 SEC AFTER AIRCRAFT

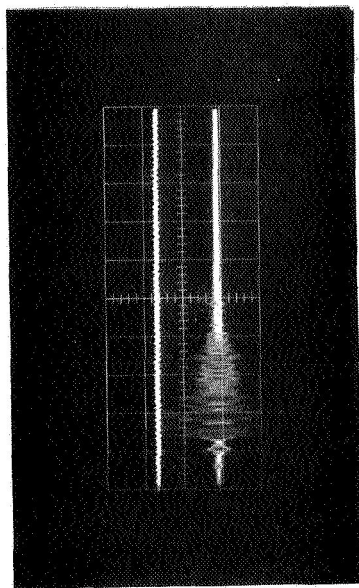


d) 6 SEC AFTER AIRCRAFT

Figure 13 RADAR RETURNS FROM RUN 54

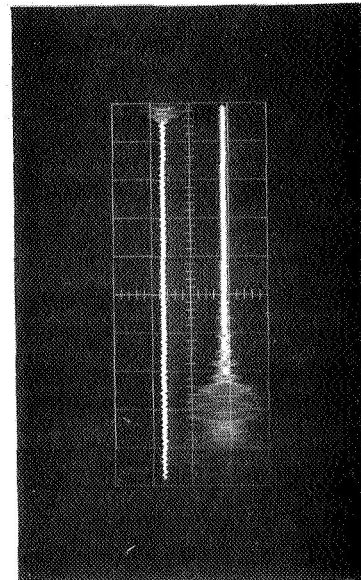


a) AIRCRAFT RETURN

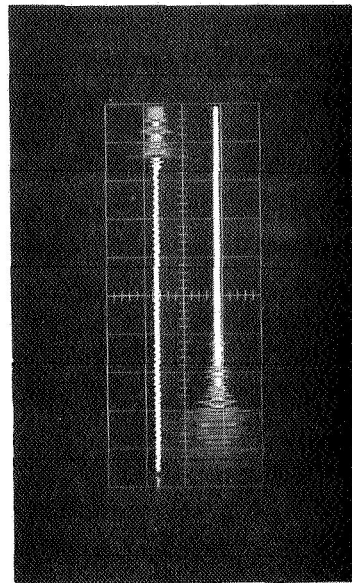


b) 2 SEC AFTER AIRCRAFT

UPPER TRACE 125 FT-175 FT
LOWER TRACE 175 FT-225 FT

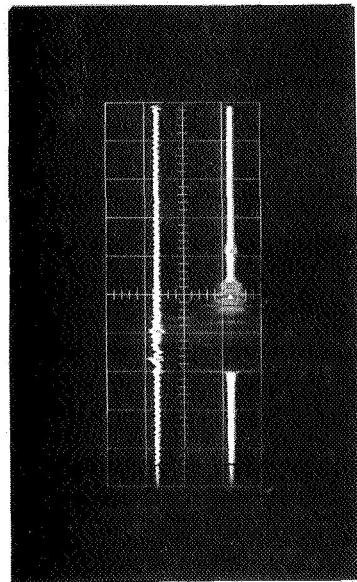


c) 3 SEC AFTER AIRCRAFT

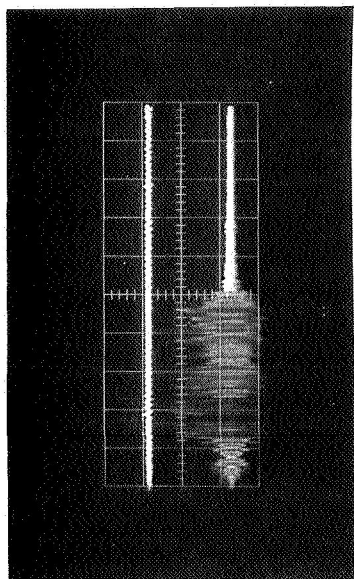


d) 4 SEC AFTER AIRCRAFT

Figure 14 RADAR RETURNS FROM RUN 47

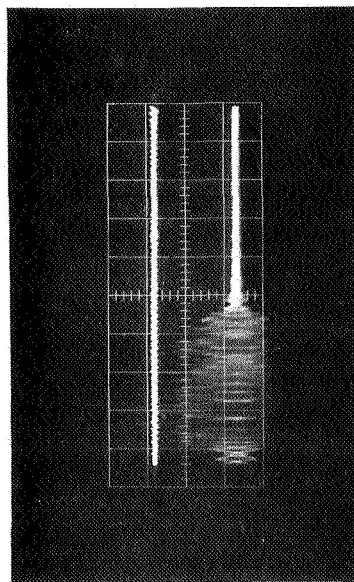


a) AIRCRAFT RETURN

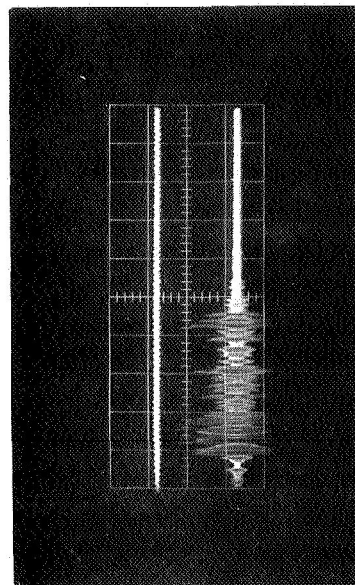


b) 4 SEC AFTER AIRCRAFT

UPPER TRACE 125 FT-175 FT
LOWER TRACE 175 FT-225 FT



c) 5 SEC AFTER AIRCRAFT



d) 6 SEC AFTER AIRCRAFT

Figure 15 RADAR RETURNS FROM RUN 56a

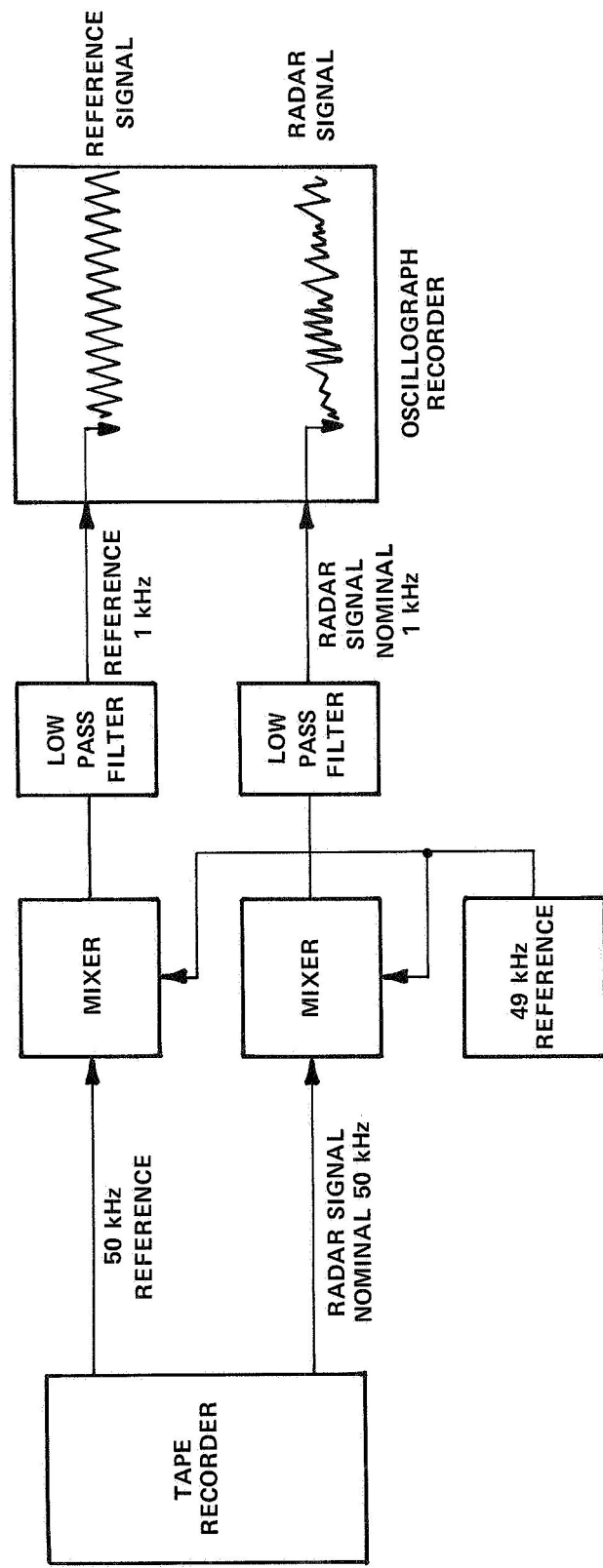


Figure 16 DIRECT STRIP CHART RECORDING OF DOPPLER SIGNAL TIME HISTORIES

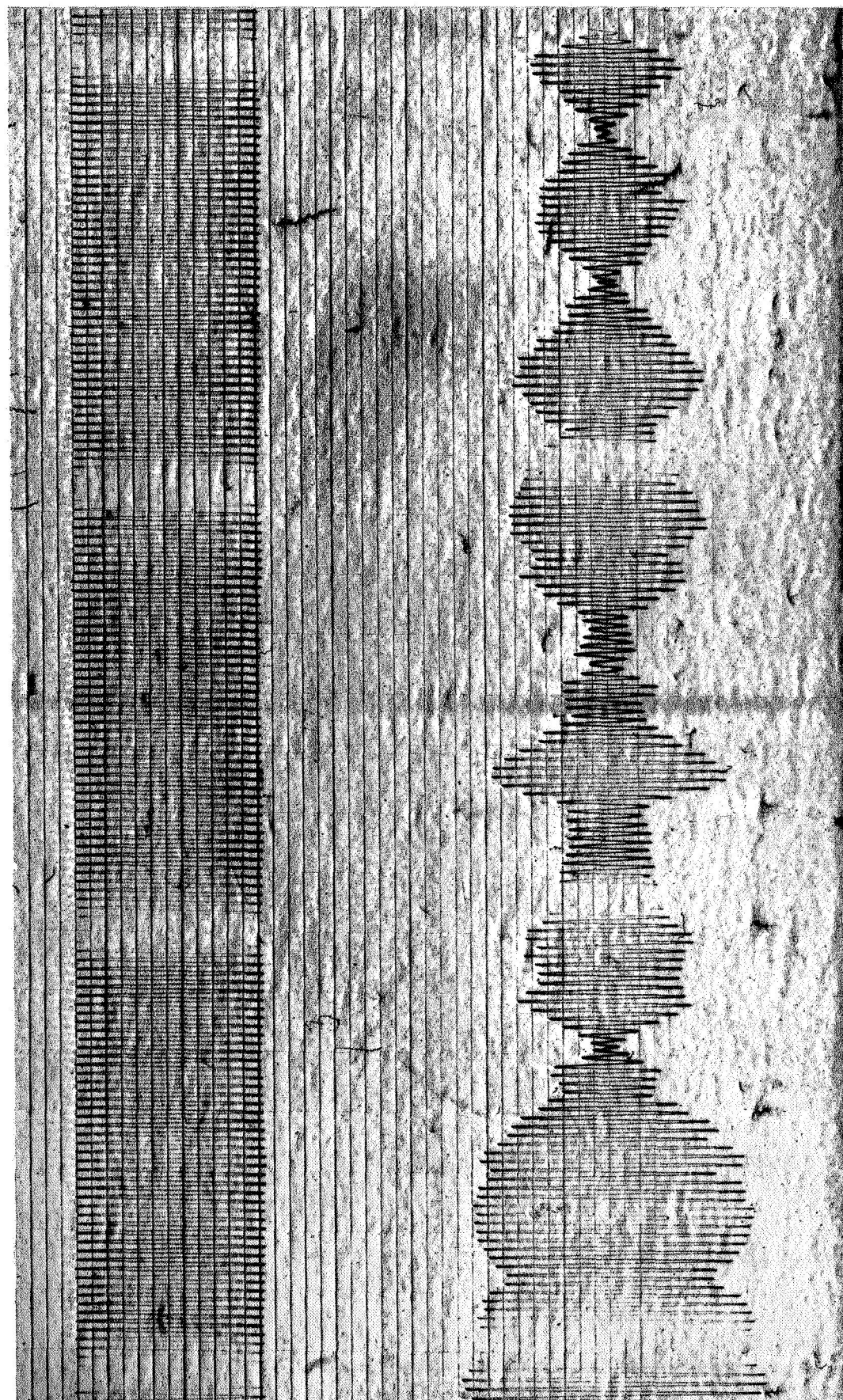


Figure 17a EXPANDED STRIP CHART RECORDING, RUN 19a
9 SEC AFTER AIRCRAFT

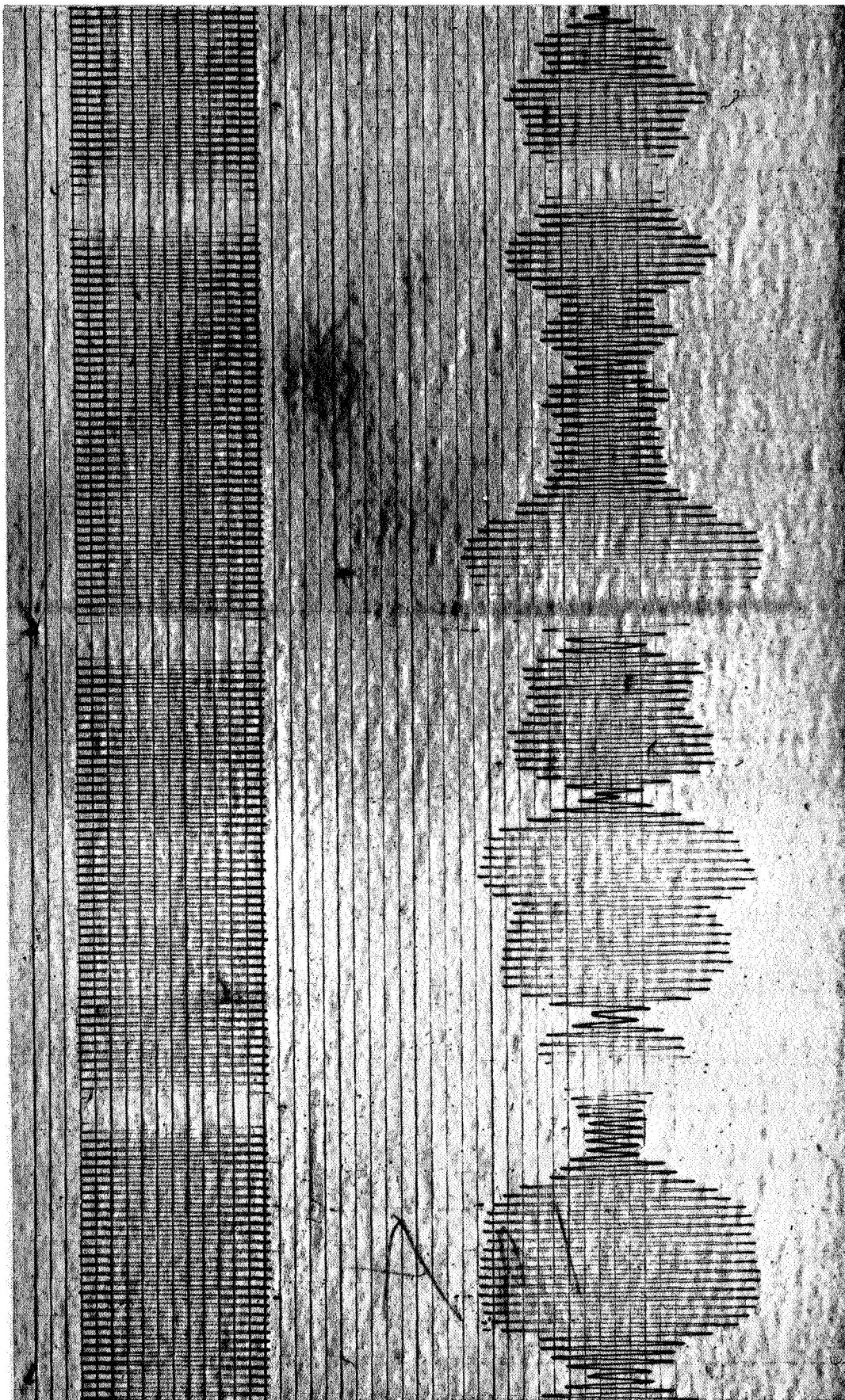


Figure 17b EXPANDED STRIP CHART RECORDING, RUN 19a
10 SEC AFTER AIRCRAFT

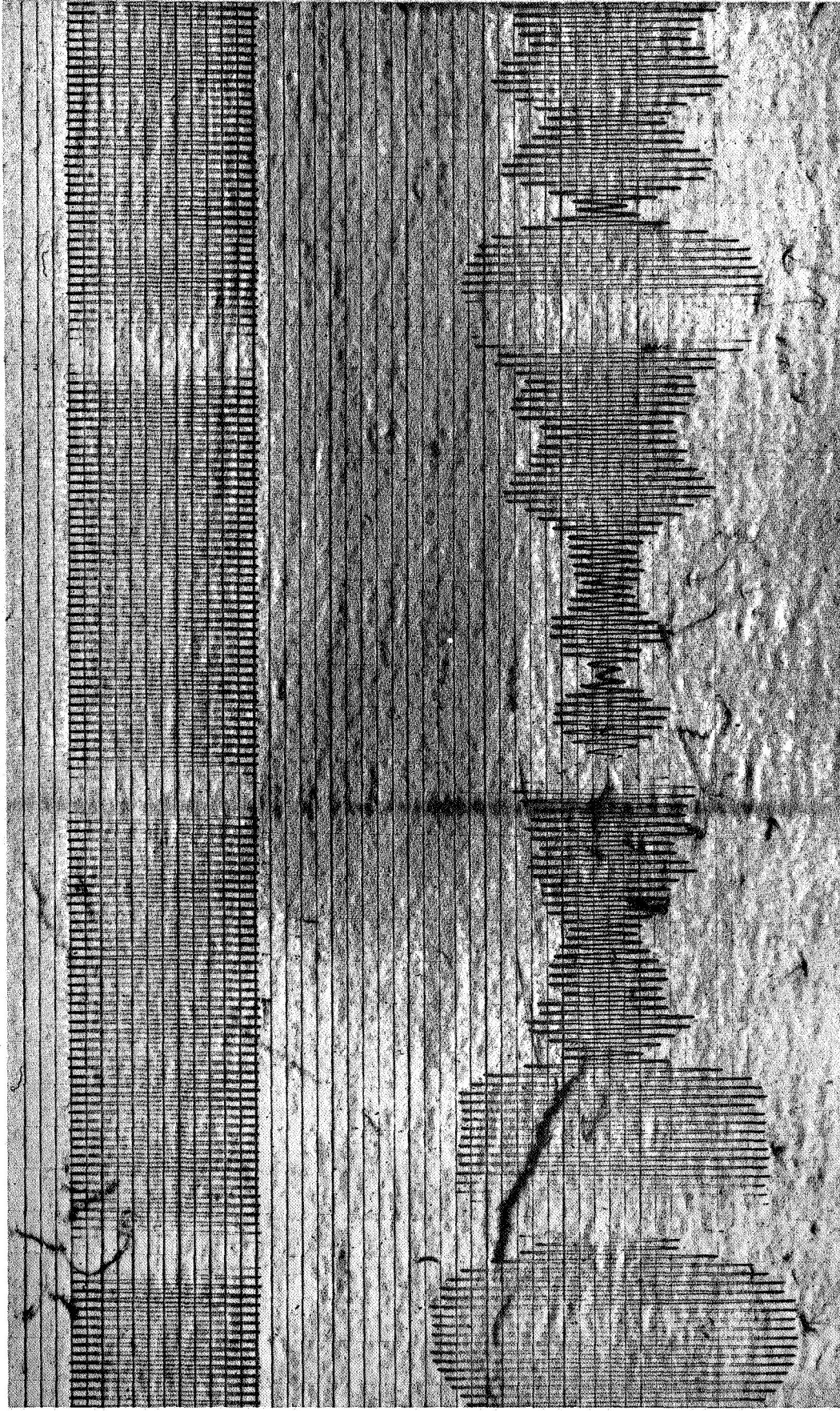


Figure 17c EXPANDED STRIP CHART RECORDING, RUN 19a
11 SEC AFTER AIRCRAFT

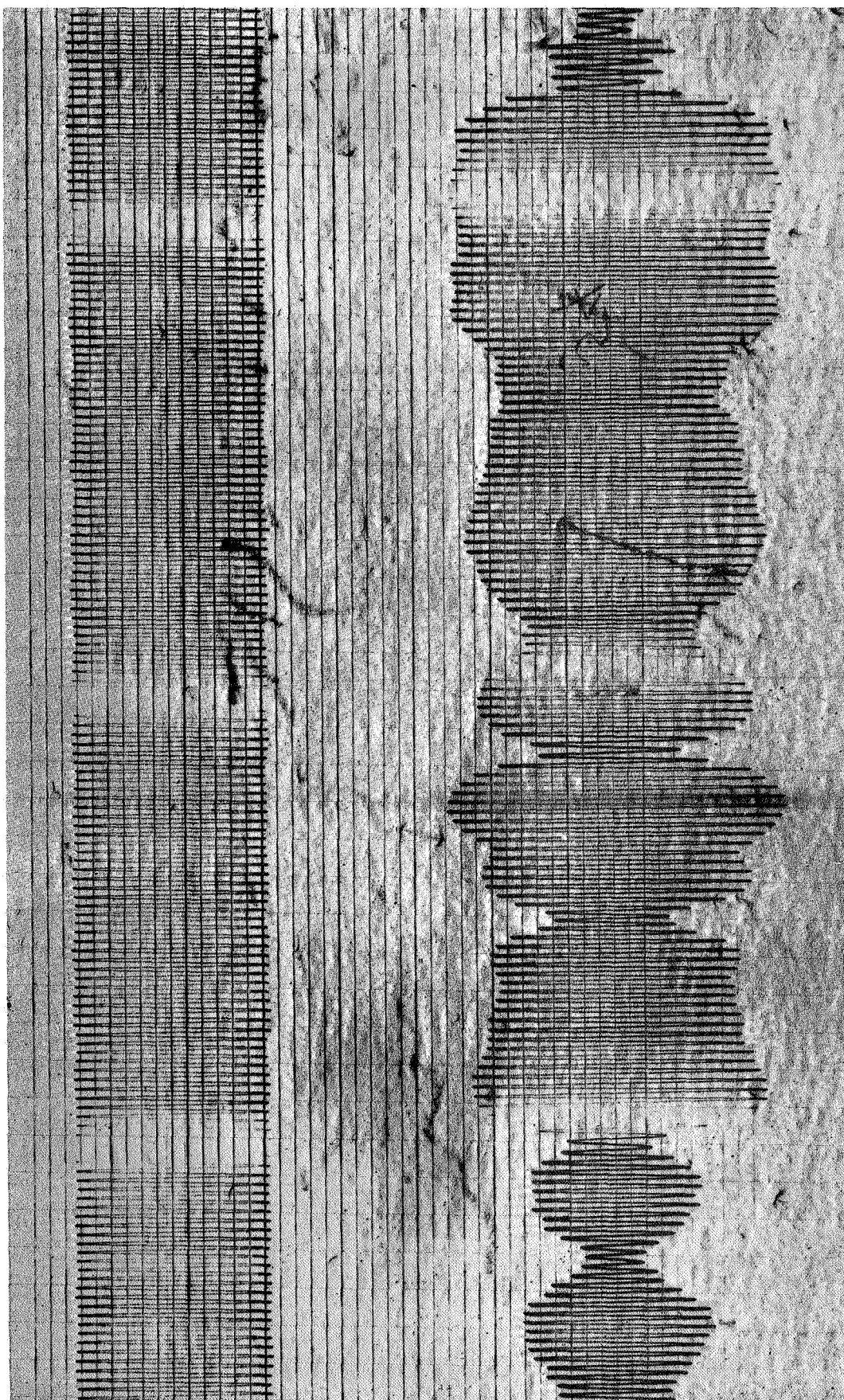


Figure 18a EXPANDED STRIP CHART RECORDING, RUN 54
4 SEC AFTER AIRCRAFT

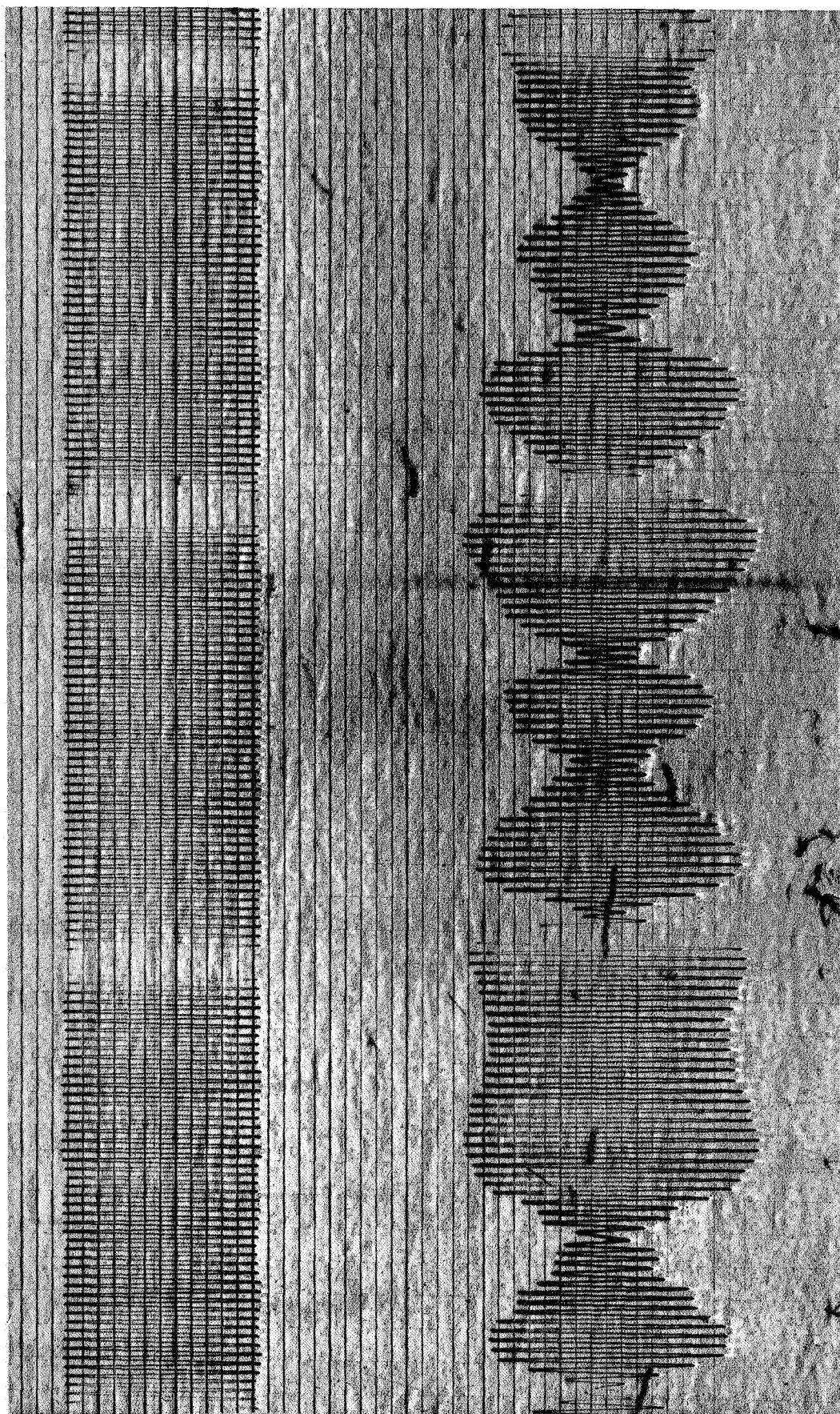


Figure 18b EXPANDED STRIP CHART RECORDING, RUN 54
5 SEC AFTER AIRCRAFT

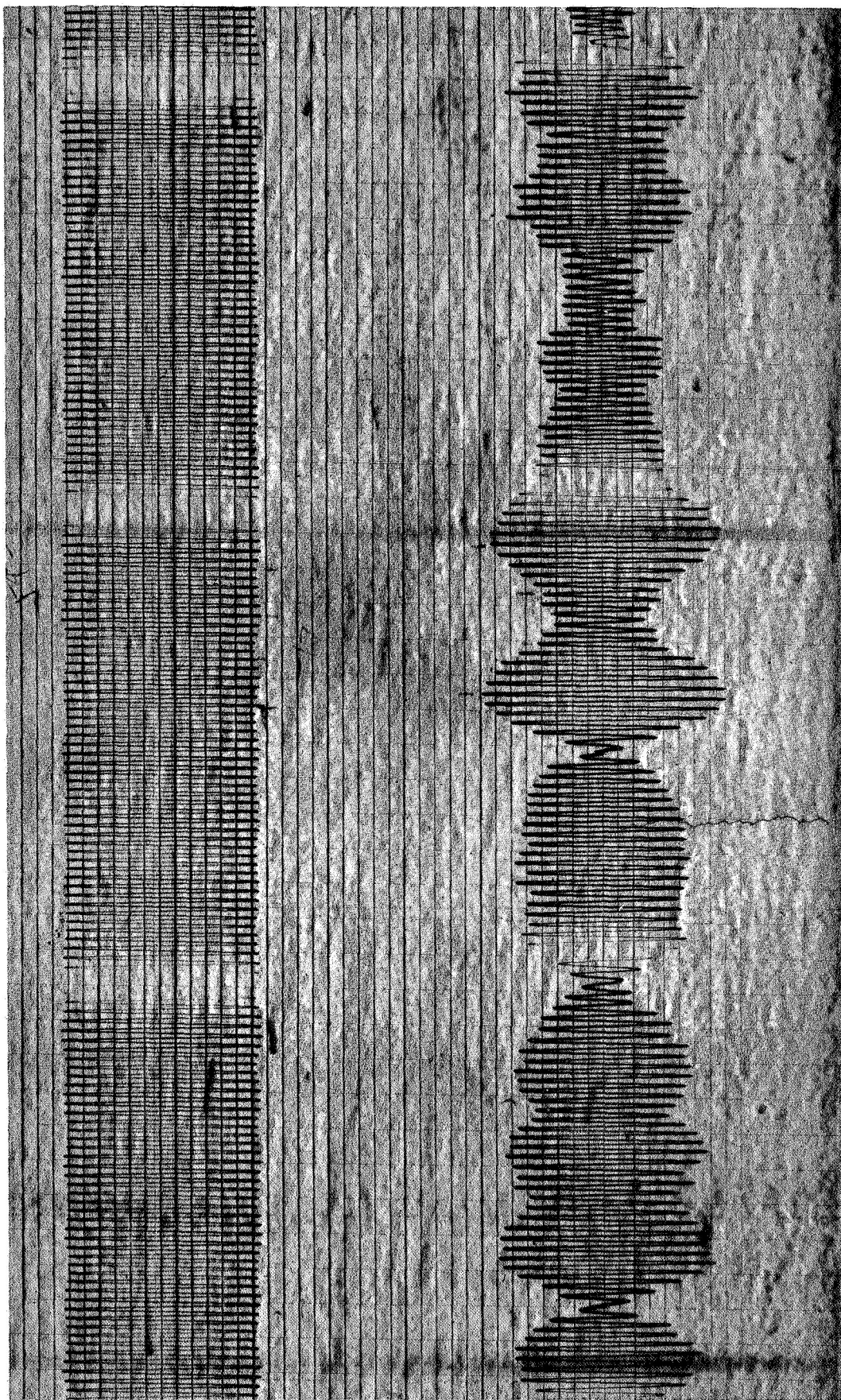


Figure 18c EXPANDED STRIP CHART RECORDING, RUN 54
6 SEC AFTER AIRCRAFT

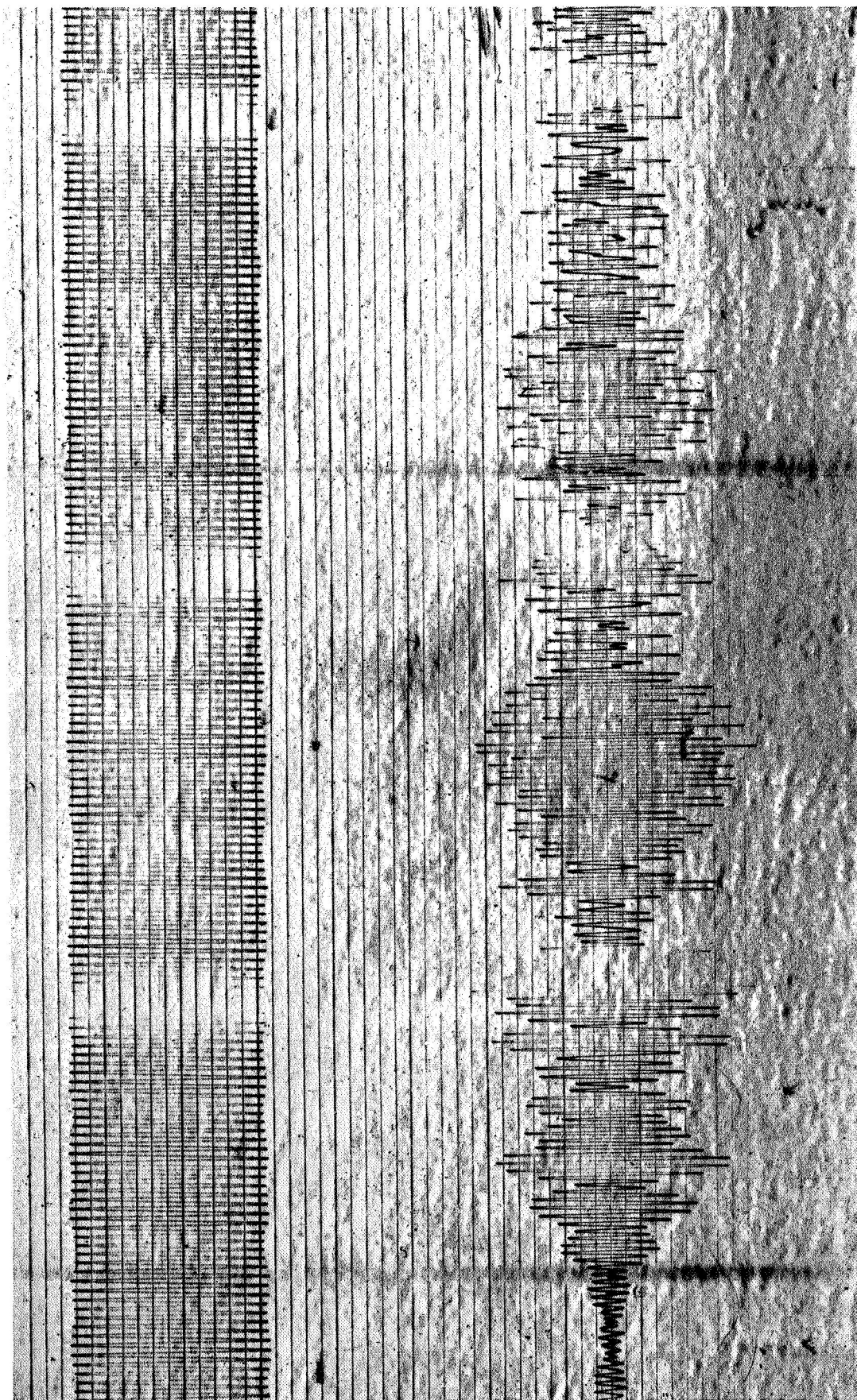


Figure 19a EXPANDED STRIP CHART RECORDING, RUN 47
2 SEC AFTER AIRCRAFT

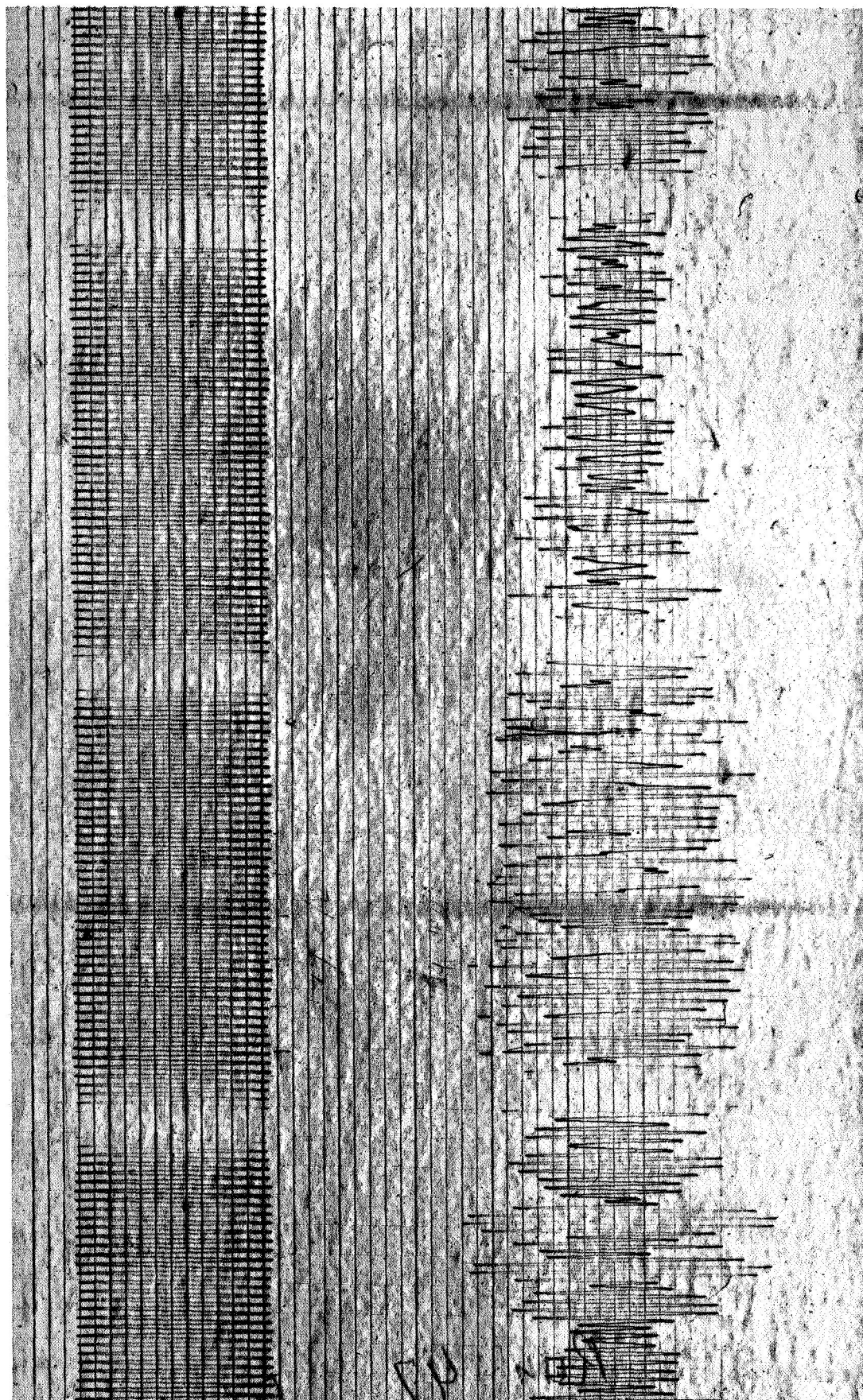


Figure 19b EXPANDED STRIP CHART RECORDING, RUN 47
3 SEC AFTER AIRCRAFT

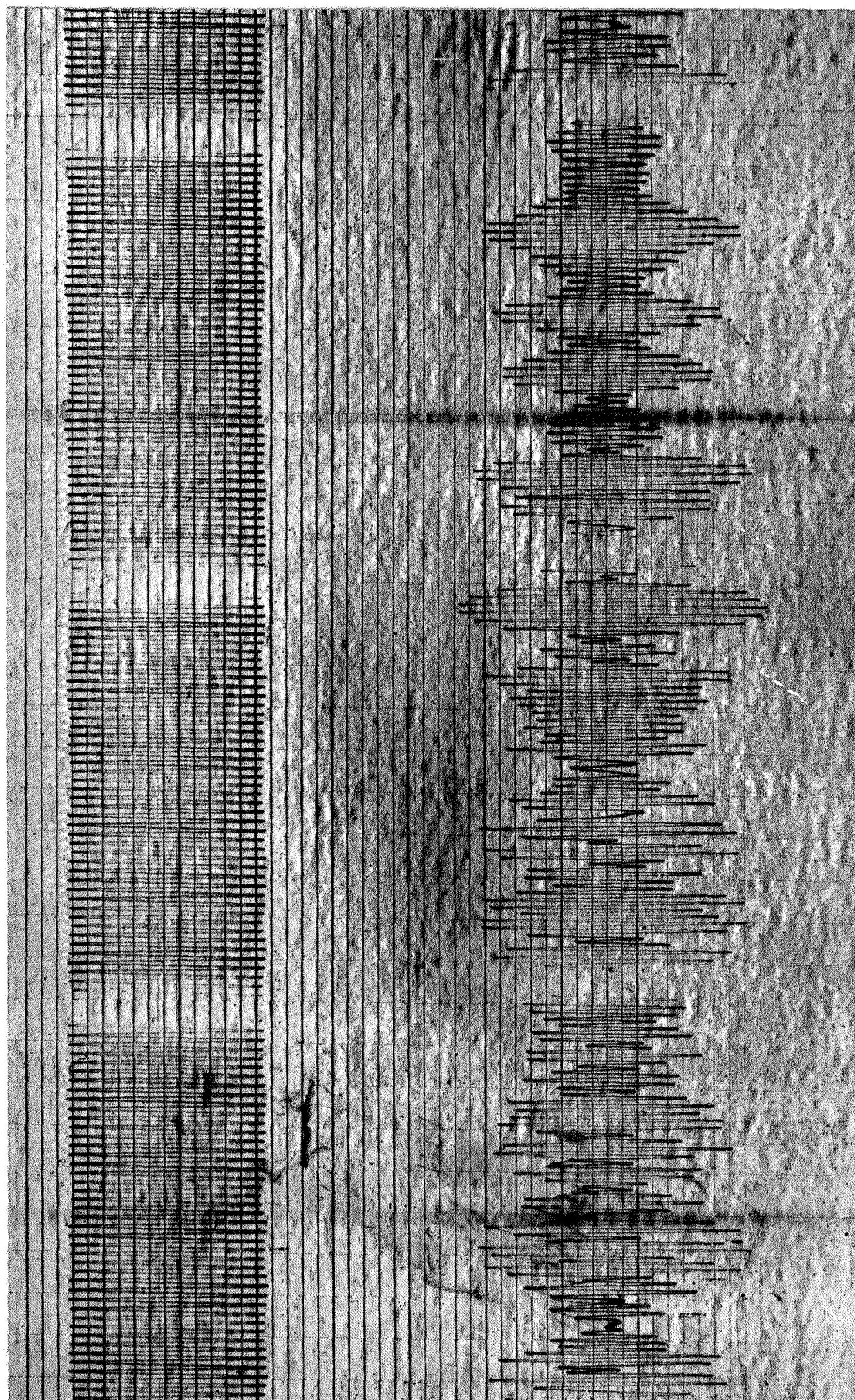


Figure 19c EXPANDED STRIP CHART RECORDING, RUN 47
4 SEC AFTER AIRCRAFT

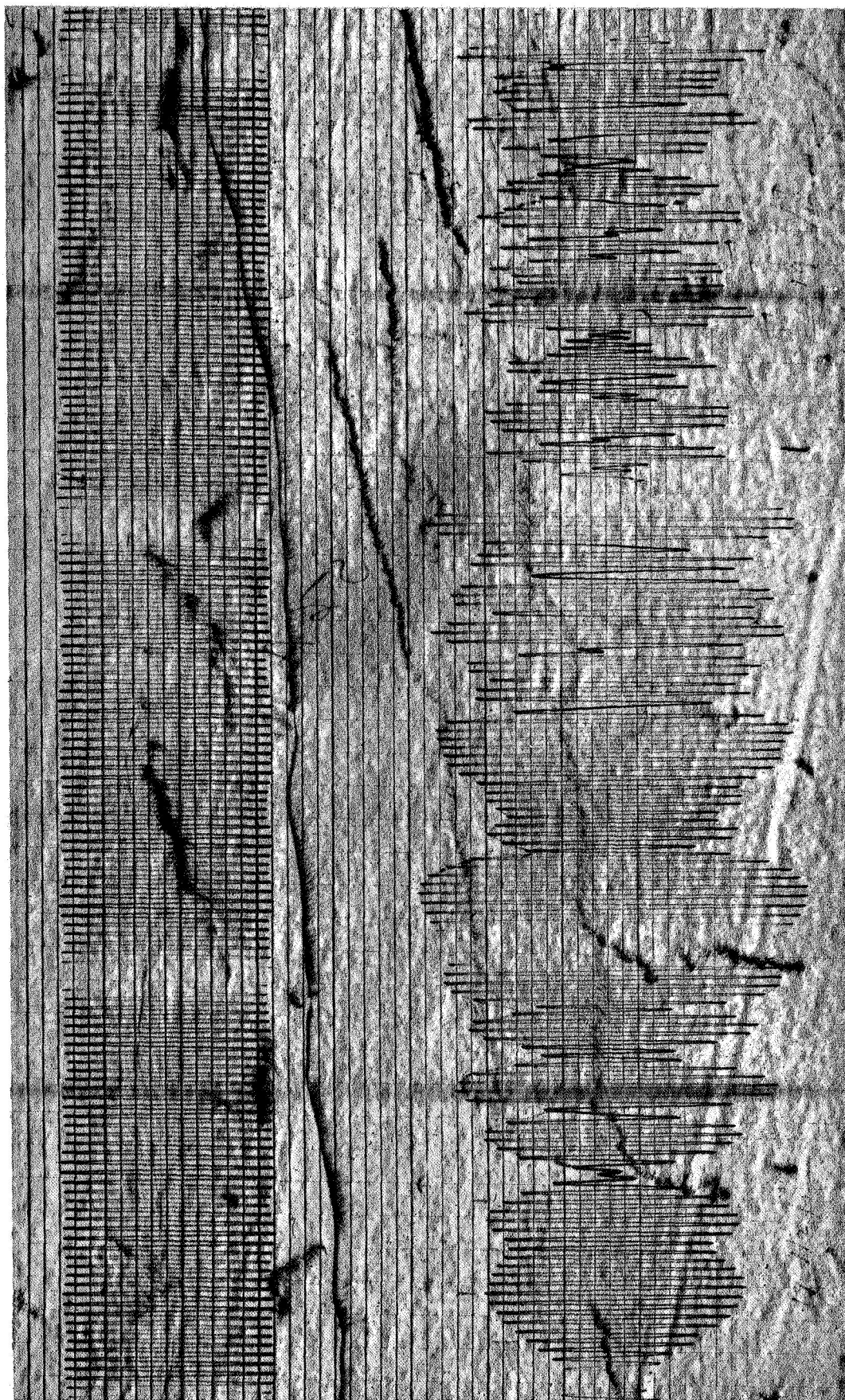


Figure 20a EXPANDED STRIP CHART RECORDING, RUN 56a
4 SEC AFTER AIRCRAFT

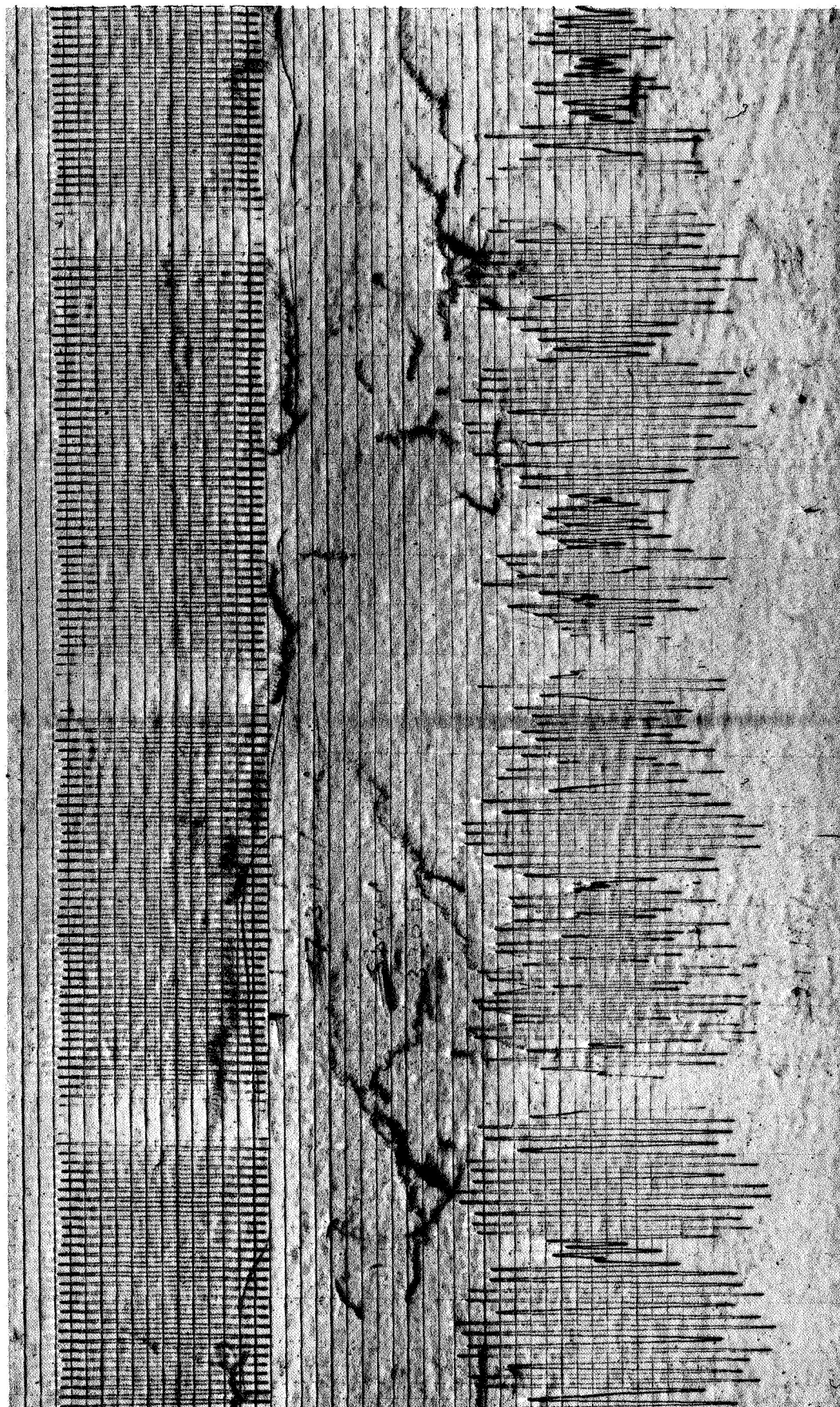


Figure 20b EXPANDED STRIP CHART RECORDING, RUN 56a
5 SEC AFTER AIRCRAFT

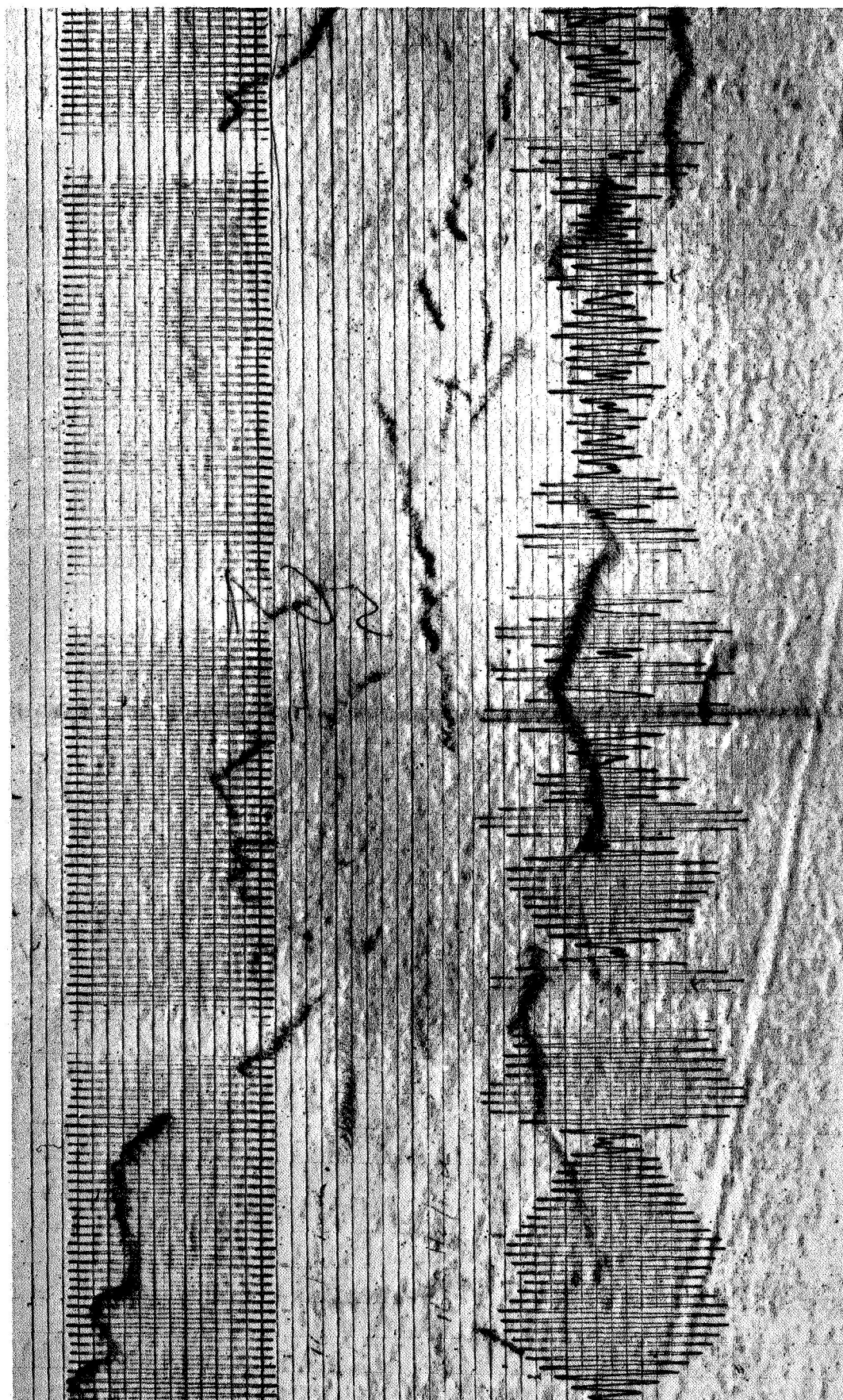
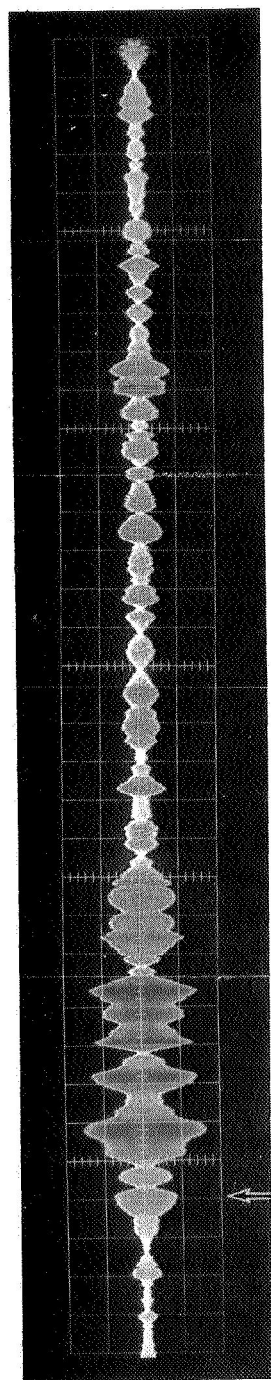
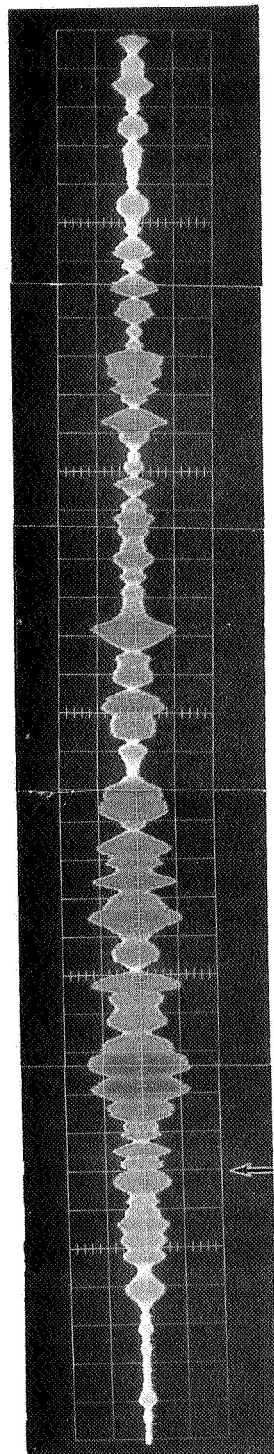


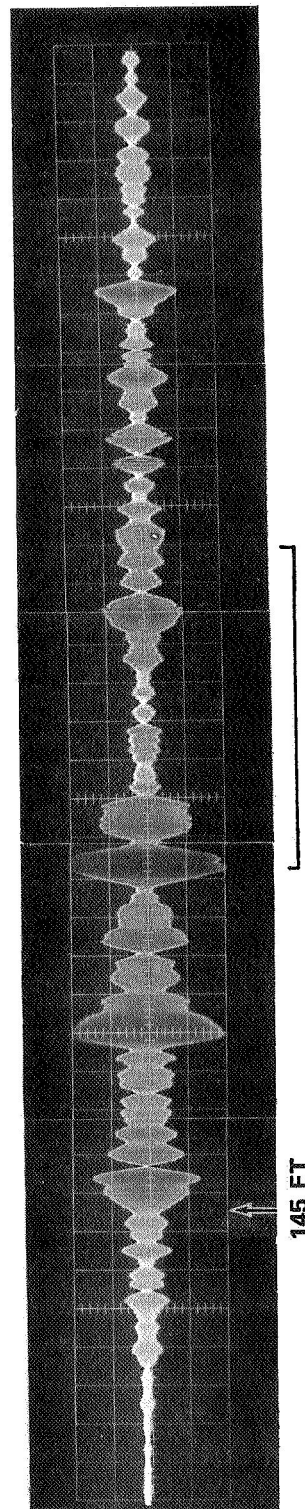
Figure 20c EXPANDED STRIP CHART RECORDING, RUN 56a
6 SEC AFTER AIRCRAFT



a) 9 SEC AFTER AIRCRAFT



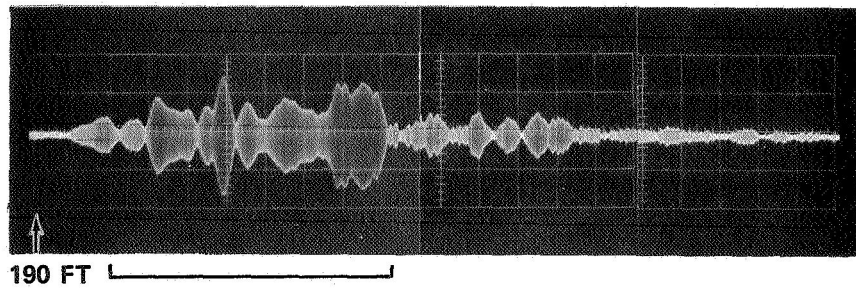
b) 10 SEC AFTER AIRCRAFT



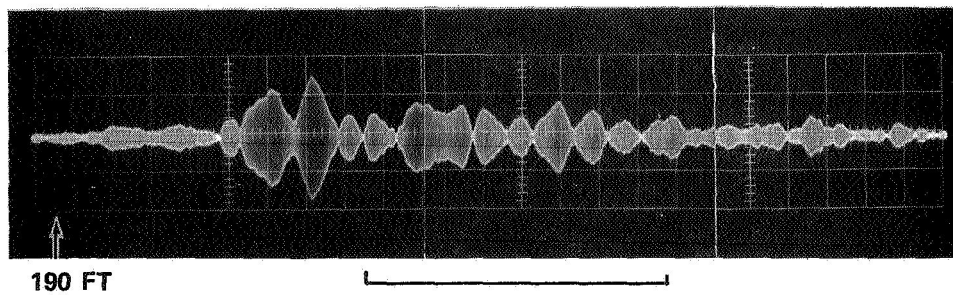
c) 11 SEC AFTER AIRCRAFT

1 HOR. DIV. = 1 FT

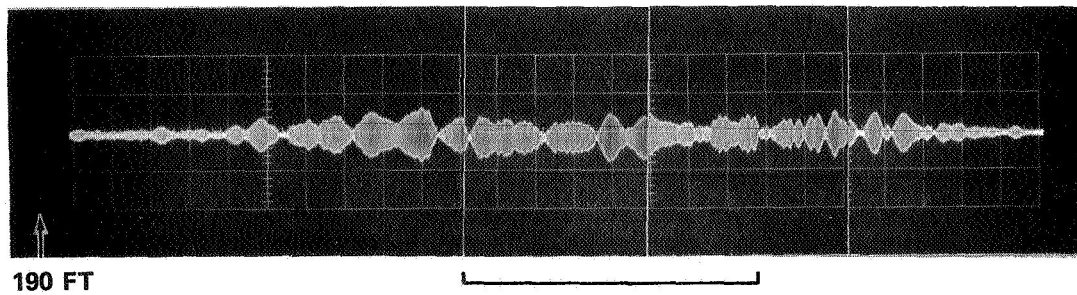
Figure 21 RUN 19a, EXPANDED OSCILLOSCOPE PHOTOGRAPHS



a) 4 SEC AFTER AIRCRAFT



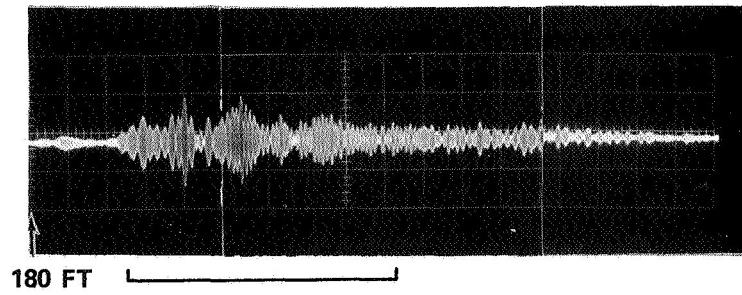
b) 5 SEC AFTER AIRCRAFT



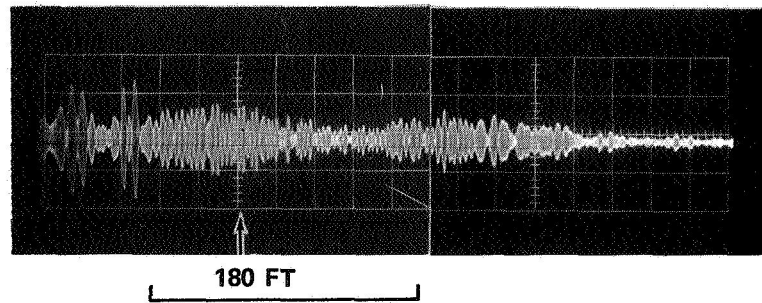
c) 6 SEC AFTER AIRCRAFT

1 HOR. DIV. = 1 FT

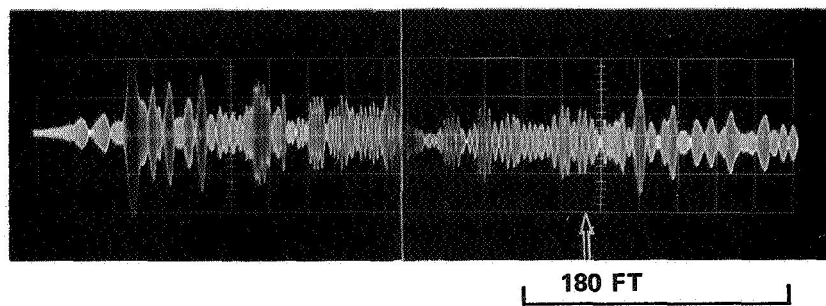
Figure 22 RUN 54, EXPANDED OSCILLOSCOPE PHOTOGRAPHS



a) 2 SEC AFTER AIRCRAFT



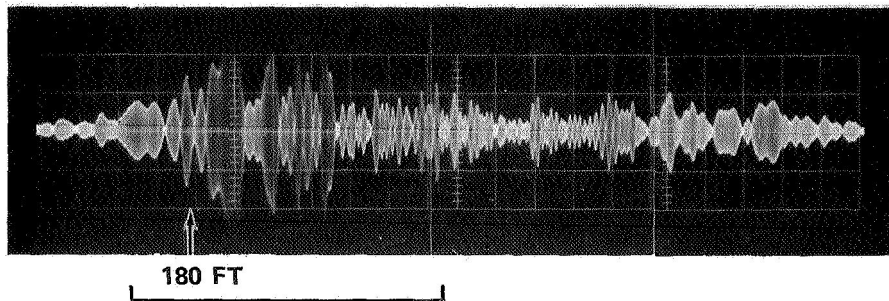
b) 3 SEC AFTER AIRCRAFT



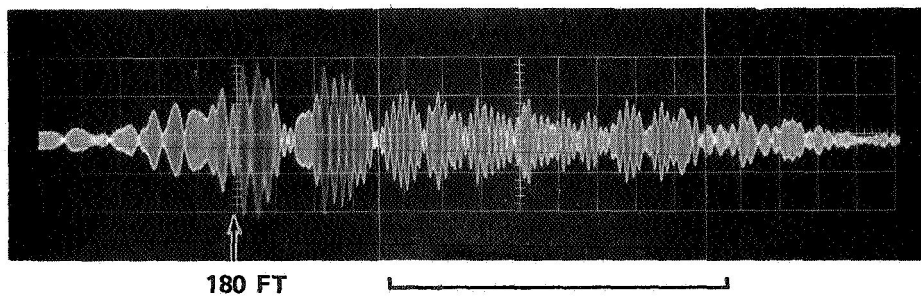
c) 4 SEC AFTER AIRCRAFT

1 HOR DIV = 1 FT.

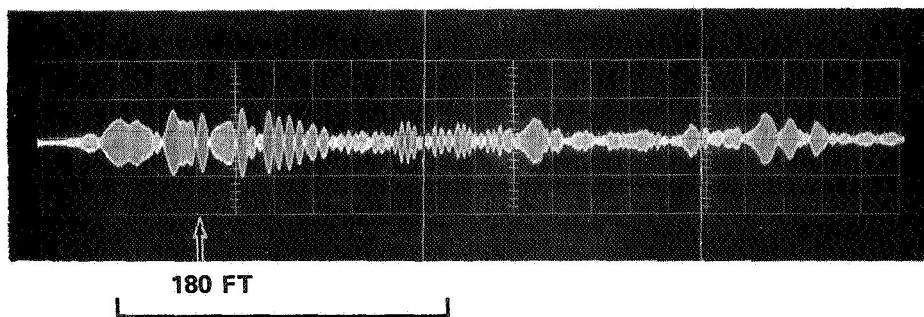
Figure 23 RUN 47, EXPANDED OSCILLOSCOPE PHOTOGRAPHS



a) 4 SEC AFTER AIRCRAFT



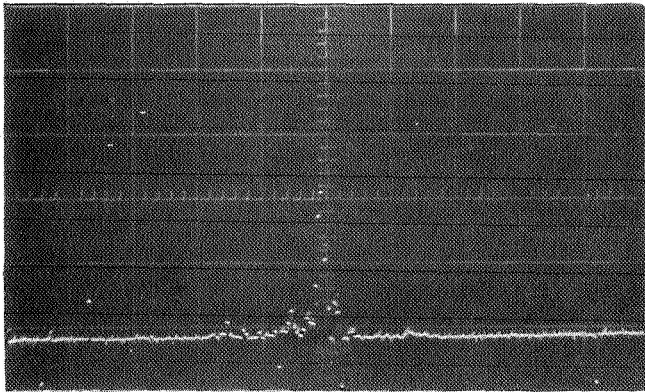
b) 5 SEC AFTER AIRCRAFT



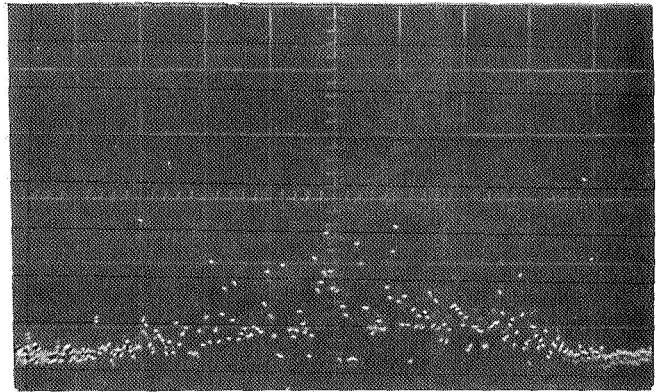
c) 6 SEC AFTER AIRCRAFT

1 HOR. DIV. = 1 FT

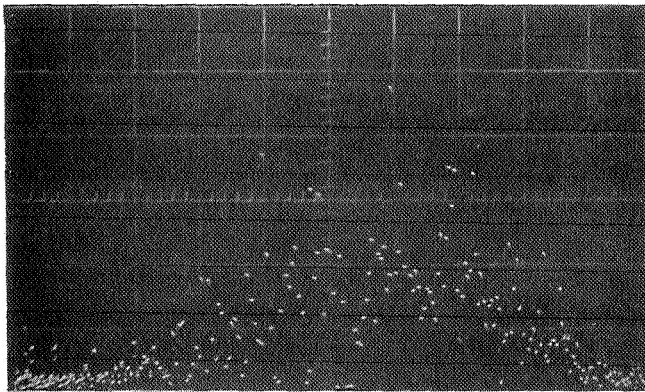
Figure 24 RUN 56a, EXPANDED OSCILLOSCOPE PHOTOGRAPHS



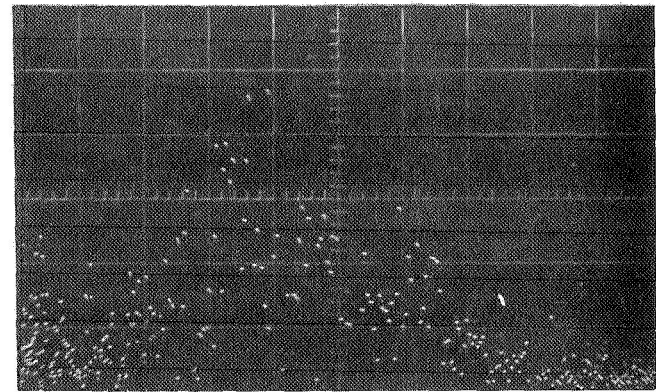
(a)



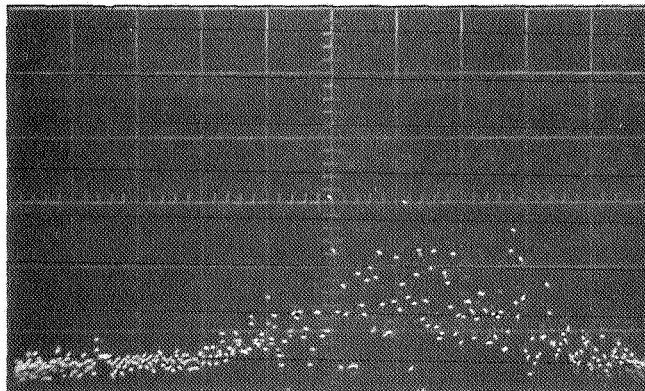
(d)



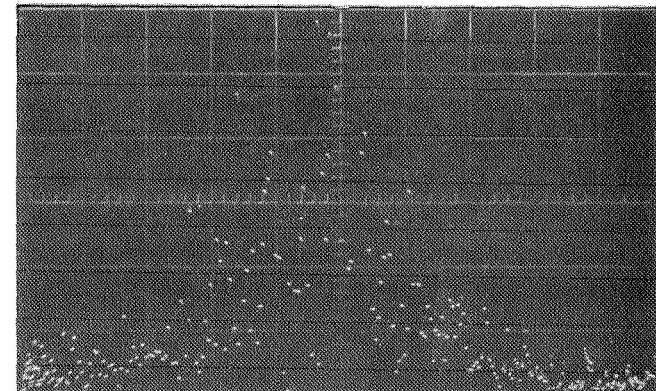
(b)



(e)



(c)



(f)

Figure 25 SPECTRUM ANALYZER RESULTS